Supporting Information for CO Coadsorption Effects on Water-Gas Shift Reaction over Cu Clusters on Cu(111): Insights from Machine Learning Force Fields and Microkinetic Modeling

Muhammad Fadhlan Anshor,[†] Harry Handoko Halim,[†,‡] and Yoshitada Morikawa[*,†,¶,‡]

†*Department of Precision Engineering, Graduate School of Engineering, The University of Osaka, 2-1 Yamadaoka, Suita, Osaka 565-0871, Japan*

‡*Innovative Catalysis Science Division, Institute for Open and Transdisciplinary Research Initiatives (ICS-OTRI), The University of Osaka, Suita, Osaka 565-0871, Japan*

¶*Research Center for Precision Engineering, Graduate School of Engineering, The University of Osaka, 2-1 Yamadaoka, Suita, Osaka 565-0871, Japan*

E-mail: morikawa@prec.eng.osaka-u.ac.jp

Contents

S1 Density Functional Theory

Adsorption energies were calculated as

$$E_{\text{ads}} = E_{\text{adsorbate+slab}} - E_{\text{adsorbate}} - E_{\text{slab}}.$$

Activation and reaction energies were defined as

$$E_a = E_{\text{TS}} - E_{\text{IS}}, \quad \Delta E = E_{\text{FS}} - E_{\text{IS}},$$

where E_{IS}, E_{TS}, and E_{FS} are the DFT energies of the initial, transition, and final states, respectively.

Table S1 shows the adsorption energy of CO on Cu(111) and Cu clusters using revPBE+D2 and revPBE. It is shown that the D2 tends to overbind CO.

Table S1: Adsorption energies (eV) of CO on Cu surfaces and clusters. For all systems, CO adsorption energies correspond to adsorption on the top site of surface or cluster Cu atoms.

Surface	revPBE	revPBE+D2	Experiment
Cu(111)	-0.48	-0.84	-0.50[1]
Cu_7	-0.83	-1.10	
Cu_4	-0.91	-1.13	
Cu_3	-0.93	-1.15	
Cu_2	-0.96	-1.12	
Cu_1	-1.00	-1.13	

Table S2 shows the activation energy of CO oxidation, carboxyl formation, and CO hydrogenation using the revPBE+D2 and revPBE on Cu(111) and Cu clusters. Overall, the difference is within the 0.1 eV.

Table S2: Activation energies (eV) of CO-related elementary steps on Cu surfaces and clusters.

	CO oxidation		Carboxyl formation		CO hydrogenation	
Surface	revPBE	revPBE+D2	revPBE	revPBE+D2	revPBE	revPBE+D2
Cu(111)	0.58	0.59	0.52	0.51	1.06	1.08
Cu_7	0.84	0.74	0.51	0.61	1.17	1.25
Cu_4	0.93	0.86	0.72	0.77	1.25	1.26
Cu_3	0.71	0.74	0.63	0.74	1.33	1.00

S2 Machine Learning Force Field Details

The details of the dataset construction, descriptors used for the MLFF, hyperparameter settings, and the accuracy of the MLFF are discussed in this section.

S2.1 Training Workflow

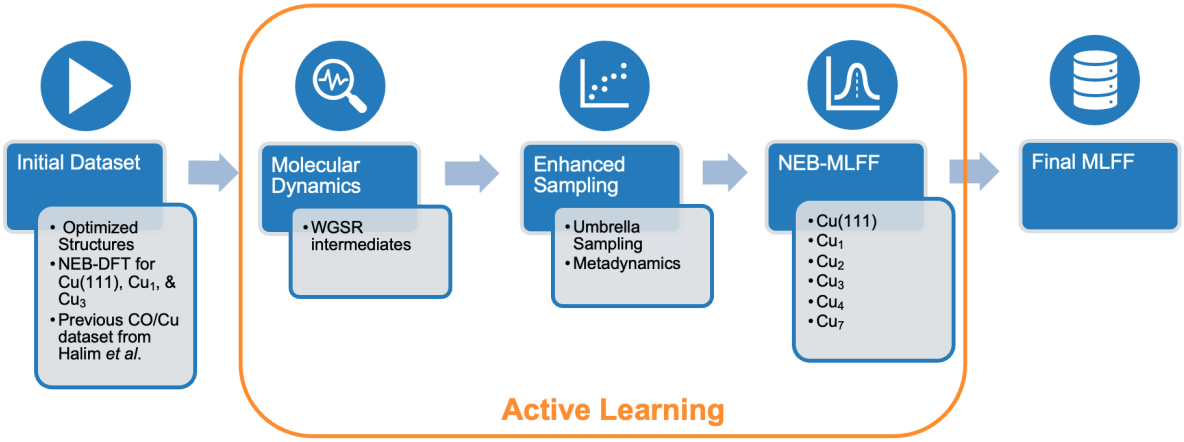

Figure S1: Dataset construction workflow

The training workflow is illustrated in Figure S1. The initial data set was generated from DFT-optimized geometries of reaction intermediates on Cu(111), Cu_1/Cu(111), and Cu_3/Cu(111). NEB calculations were performed to obtain the corresponding transition states. We also added some portion of the previous CO-Cu dataset which have been used to

perform the machine learning molecular dynamics (MLMD) simulation of CO-induced Cu cluster formation on Cu(111).[2] An active learning approach was done in three steps, molecular dynamics (MD) for WGSR intermediates, enhanced sampling to obtain more transition states of WGSR elementary steps, and NEB-MLFF to confirm the transition state by finding the one imaginary frequency via the vibrational modes calculation. The MD and the enhanced simulations is done via the LAMMPS code[3] and PLUMED.[4,5] The NEB-MLFF is done using the Atomistic Simulation Environment (ASE).[6] An initial MLFF was trained and then used to perform umbrella sampling and metadynamics to further collect structures near the transition state on Cu(111), Cu_1–Cu_4, and Cu_7 surfaces. These structures were refined by DFT single-point energy calculations and iteratively added to the training database. The updated MLFF was used to perform NEB calculations on Cu_2, Cu_4, and Cu_7 systems. DFT single-point calculations were again used to calculate the activation energy and reaction energy. If the agreement between DFT and MLFF is larger than 0.1 eV, then the corresponding structures will be added to the dataset and once again update the MLFF. The final MLFF was then used to perform NEB and vibrational analysis for all systems, and the IS, TS, and FS structures were taken to validate the activation energy. This workflow significantly reduced the number of expensive DFT-NEB calculations required.

S2.2 GAP Hyperparameters

To build the MLFF we use the Gaussian Approximation Potential (GAP)[7] in combination with turbo SOAP[8] as our many body descriptor and a 2-body descriptor as listed in Table S3

Table S3: Descriptors used in MLFF training

Descriptor	**Cutoff**	**N sparse**	**delta**	**sparse method**	**nmax**	**lmax**
2 body	4.5 Å	50	2.0	uniform		
soap_turbo for Cu	4 Å	3500	0.1	cur_points	7	4
soap_turbo for C, H, O	4 Å	7000	0.1	cur_points	7	4
soap_turbo for C, H, O	6 Å	7000	0.1	cur_points	7	4

For the GAP setting, we set the *default_sigma* for energy, forces, and hessians to be 0.001, 0.01, 0.01, 0.0, respectively. We add additional kernel regularization specifically for the isolated atom as *config_type_sigma*={*isolated_atom:0.0001:0.01:1.0:0.0*}.

S2.3 MLFF Training and Validation

The final dataset consist of 7286 structures. The validation set consist of 1350 structures comes from molecular dynamics and metadynamics simulation. The accuracy of the MLFF in the training set is shown in Figure S2 for energy and forces and Figure S3 for the forces of each element.

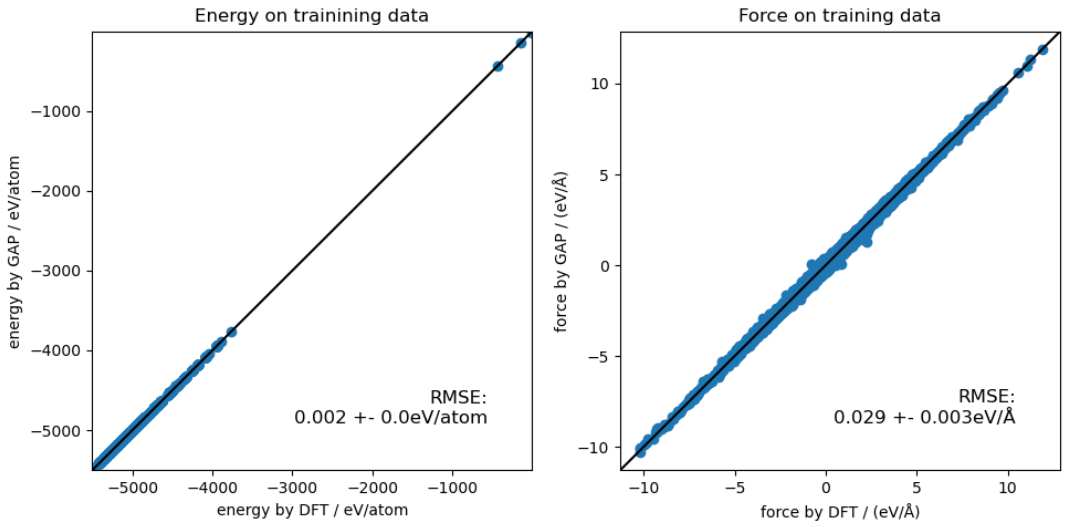

Figure S2: Parity plot for energy and forces in training set

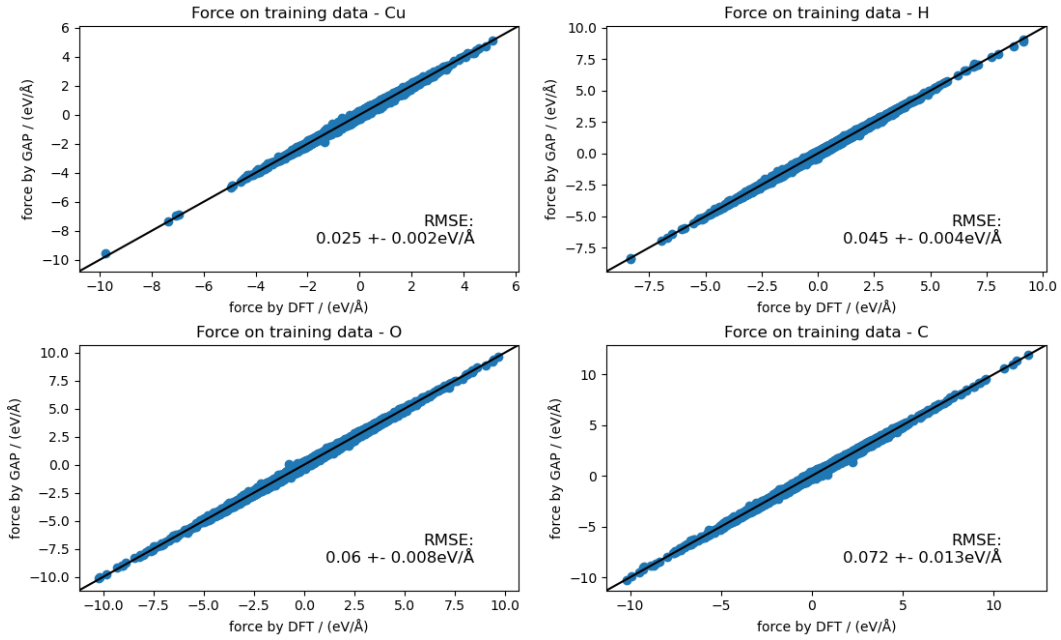

Figure S3: Parity plot for forces on each element in training set

The accuracy of the MLFF in the validation set is shown in Figure S4 for energy and forces and Figure S5 for the forces of each element.

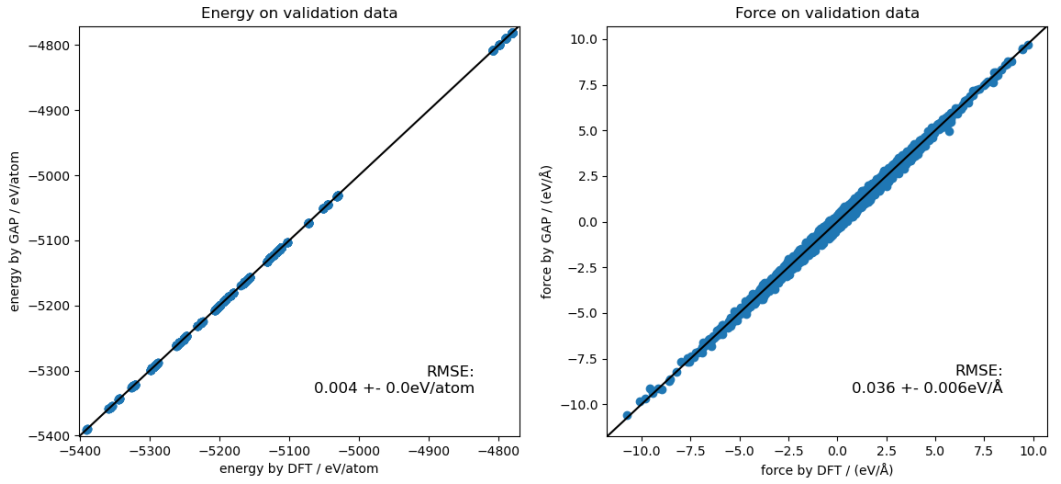

Figure S4: Parity plot for energy and forces in validation set

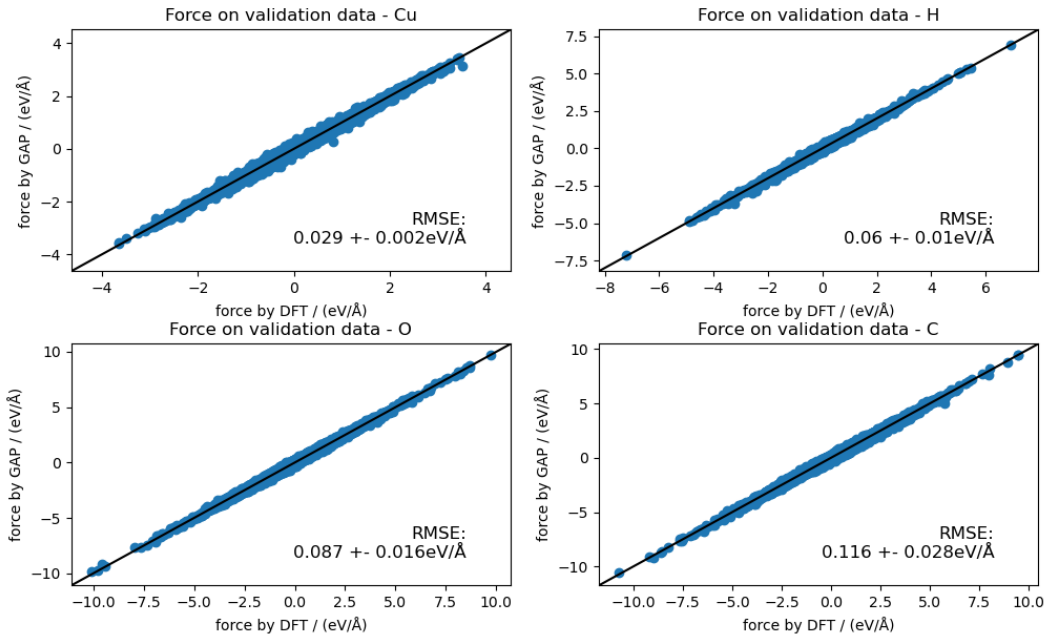

Figure S5: Parity plot for forces on each element in validation set

The MLFF is further validated to predict the activation energy and reaction energy via NEB calculations for all WGSR elementary steps across low to high CO coverages. Figure S6 shows the parity plot between GAP and DFT for activation and reaction energies. Although there are some outliers in the plot, at the end, the DFT energies are used in the microkinetic modeling.

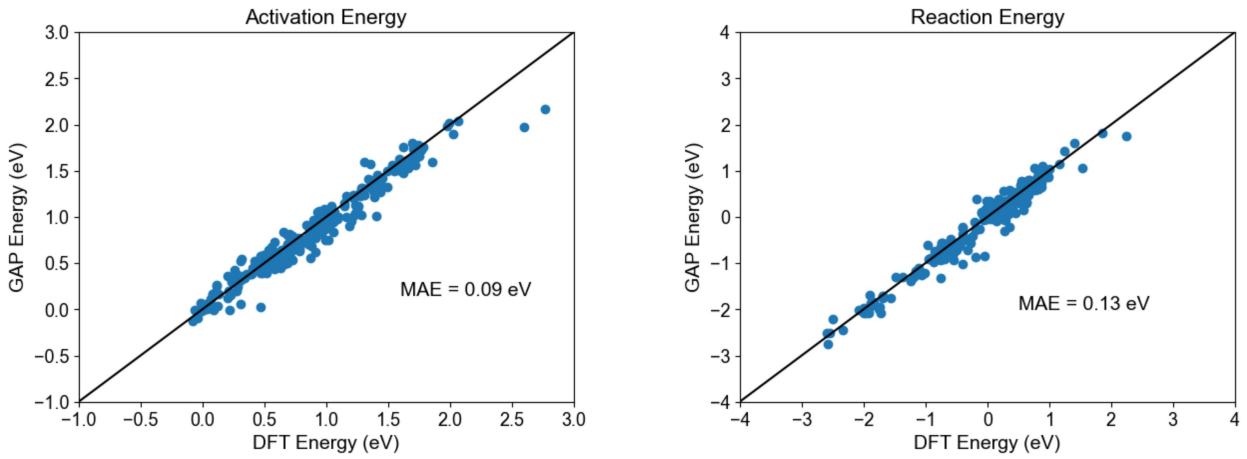

Figure S6: Parity plot for (a) activation energy and (b) reaction energy

Table S4 shows the comparison of water dissociation barriers between GAP and DFT under conditions without CO coadsorption and at high CO coverage. For Cu(111), the CO coverage is 6/16 ML; for Cu_7, 6/7 ML; for Cu_4, 3/4 ML; and for Cu_3, 2/3 ML.

Table S4: DFT and GAP energy barriers (in eV) for water dissociation on Cu surfaces with and without CO coadsorption, along with mean absolute errors (MAE).

Surface	Energy barrier (eV)				MAE
	No CO		With CO		
	DFT	GAP	DFT	GAP	
Cu(111)	1.37	1.29	1.49	1.45	0.06
Cu_7	0.69	0.60	1.05	0.93	0.11
Cu_4	0.73	0.67	1.06	0.94	0.09
Cu_3	0.84	0.79	0.94	0.74	0.13
Average					0.10

S3 MD and Enhanced Sampling Simulations

The settings and parameters for molecular dynamics (MD), umbrella sampling, and metadynamics used during the active learning phase and for constructing the validation set are described in this section.

S3.1 General Setup

All MD and enhanced sampling simulations were carried out using LAMMPS[3] and PLUMED.[5] The canonical (NVT) ensemble was employed at temperatures between 400–550 K, controlled by a Nosé–Hoover thermostat. A timestep of 0.5 fs was used. Each trajectory was equilibrated for 10 ps prior to data collection. Bias potentials were applied on selected collective variables (CVs) to explore rare events.

S3.2 Umbrella Sampling

Umbrella sampling was employed for selected elementary steps by restraining the CV around fixed reference values with harmonic biasing potentials:

$$V_{\text{bias}}(s) = \tfrac{1}{2}\kappa(s - s_0)^2,$$

where s is the CV, s_0 the reference value, and κ the force constant. A series of overlapping windows were generated along the reaction coordinate with spacing of 0.2∼0.3 Å. The value of κ varied depending on the CV and reaction (Table S5). Each window was simulated for 10-15 ps, and the unbiased free energy profile was reconstructed using the weighted histogram analysis method (WHAM).[9]

S3.3 Metadynamics

For reactions with complex reaction coordinates, well-tempered metadynamics[10] was performed. Gaussian bias potentials were deposited along the CV according to

$$V_{\mathrm{meta}}(s,t) = \sum_{t'<t} w \exp\left[-\frac{(s - s(t'))^2}{2\sigma^2}\right] \exp\left(-\frac{V(s,t')}{k_B \Delta T}\right),$$

where w is the initial Gaussian height, σ the Gaussian width, and ΔT the bias factor. Biasing parameters (w, σ, deposition stride) were chosen to balance efficient exploration and smooth convergence of the free energy surface.

S3.4 Simulation Parameters

Table S5 summarizes the CVs and umbrella/metadynamics parameters used in this work.

Table S5: Collective variables and enhanced sampling parameters. The values of κ were varied depending on the system.

Reaction	CV	Spacing (Å)	Windows	κ (eV/Å^2)
$H_2O^* \rightarrow OH^* + H^*$	O–H distance	0.2∼0.3	8	16–20.7
$OH^* \rightarrow O^* + H^*$	O–H distance	0.2∼0.3	8	18.1–31.1
$CO^* + O^* \rightarrow CO_2$	C–O distance	0.2∼0.3	8	15.5–23.3
$CO^* + OH^* \rightarrow COOH^*$	C–O distance	0.2∼0.3	8	15.5–18.1
$COOH^* \rightarrow CO_2^* + H^*$	O–H distance	0.2∼0.3	8	15.5–18.1
$CO^* + H^* \rightarrow CHO^*$	C–H distance	0.2∼0.3	8	18.1–20.7
$CHO^* + O^* \rightarrow HCOO^*$	C–O distance	0.2∼0.3	8	17.6–20.7
$HCOO^* \rightarrow CO_2^* + H^*$	C–H distance+O-C-O angle	0.2∼0.3	8	15.5–20.7
$2H^* \rightarrow H_2(g)$	H–H distance	0.2∼0.3	8	15.5–18.1

S4 WGSR Elementary Step Geometries

The elementary steps of WGSR and the corresponding reaction numbering used in this study are listed below.

R1 : $CO(g) \rightarrow CO^*$; $H_2O(g) \rightarrow H_2O^*$ (adsorption)

R2 : $H_2O^* \rightarrow OH^* + H^*$ (water dissociation)

R3 : $OH^* \rightarrow O^* + H^*$ (OH dissociation)

R3* : $2OH^* \rightarrow O^* + H_2O^*$ (OH disproportionation)

R4 : $CO^* + O^* \rightarrow CO_2^*$ (CO oxidation)

R5 : $CO^* + OH^* \rightarrow$ cis-COOH* (cis-COOH formation)

R6a : cis-COOH* $\rightarrow$ trans-COOH* (carboxyl isomerization)

R6b : trans-COOH* $\rightarrow CO_2^* + H^*$ (direct carboxyl decomposition)

R6b* : trans-COOH* + $OH^* \rightarrow CO_2^* + H_2O^*$ (OH-assisted carboxyl decomposition)

R7 : $CO^* + H^* \rightarrow CHO^*$ (CHO formation)

R8 : $CHO^* + O^* \rightarrow HCOO^*$ (formate formation)

R9 : $HCOO^* \rightarrow CO_2^* + H^*$ (formate decomposition)

R10 : $2H^* \rightarrow H_2(g)$ (H recombination)

R11 : $CO_2^* \rightarrow CO_2(g)$ (CO_2 desorption)

Figures S7–S10 show the initial states, transition states (indicated by "$\cdots$"), and final states for all elementary steps of the WGSR on clean Cu(111) and Cu clusters.

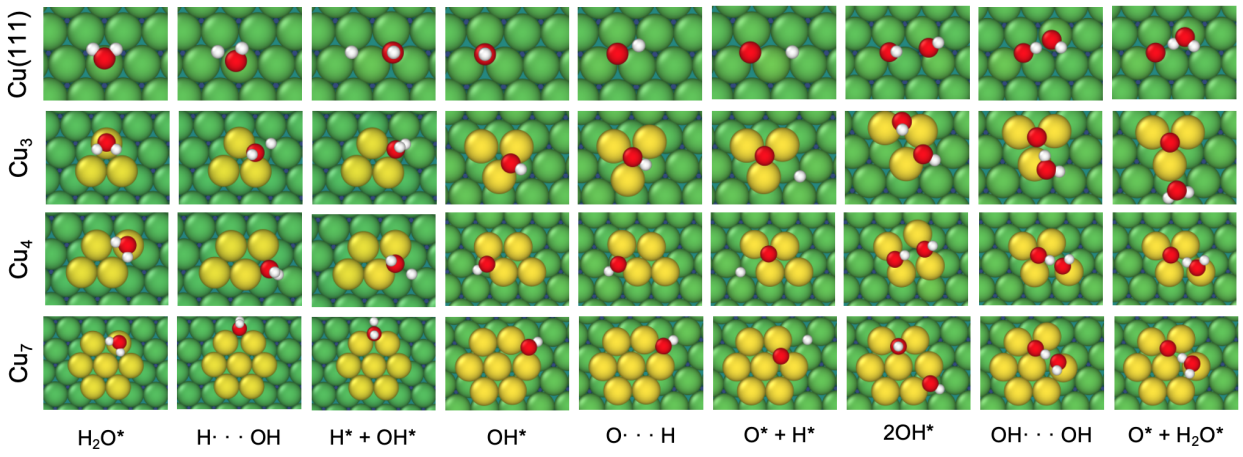

Figure S7: IS, TS, and FS of R2, R3, and R3* on Cu(111), Cu_3, Cu_4, and Cu_7

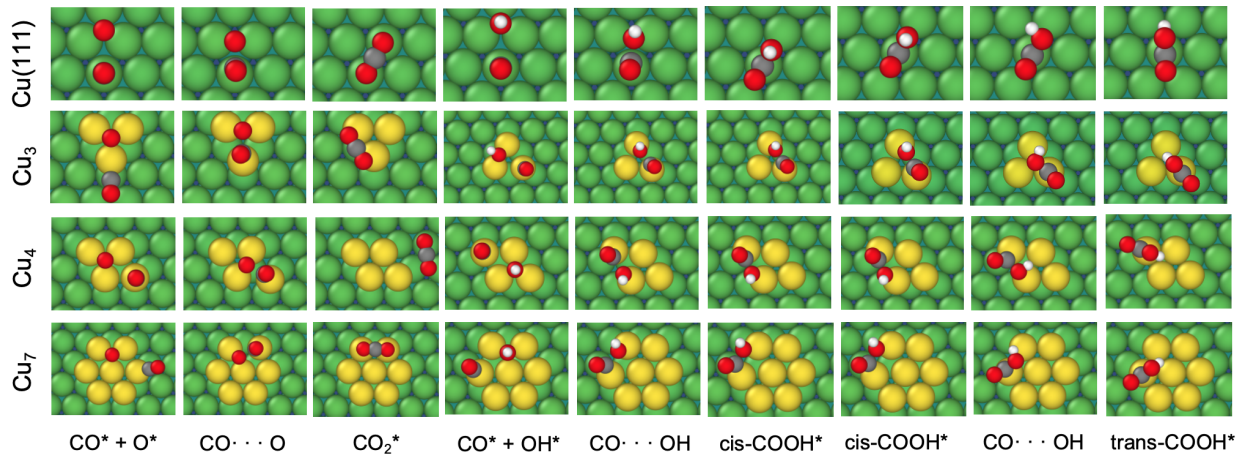

Figure S8: IS, TS, and FS of R4, R5, and R6a on Cu(111), Cu_3, Cu_4, and Cu_7

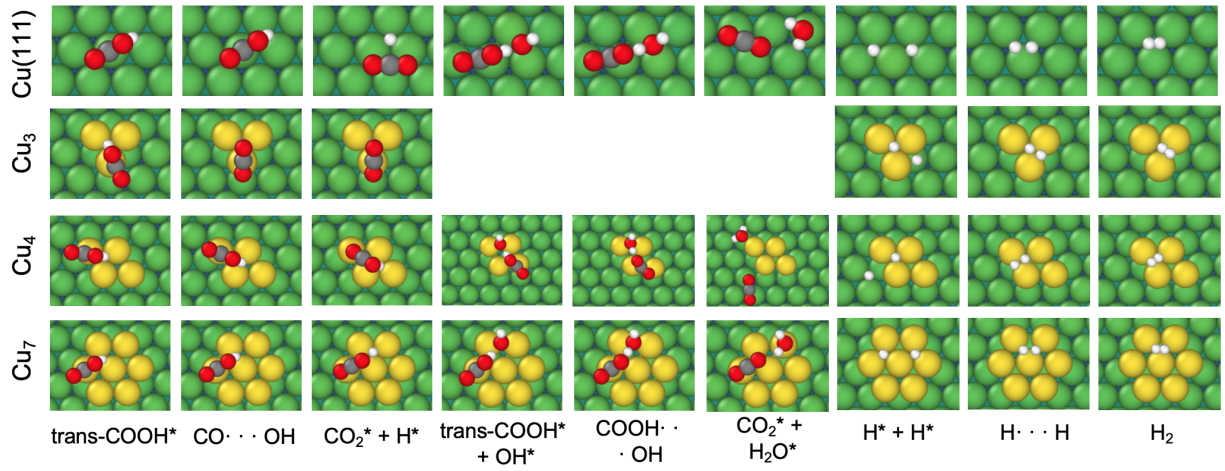

Figure S9: IS, TS, and FS of R6b, R6b*, and R10 on Cu(111), Cu_3, Cu_4, and Cu_7

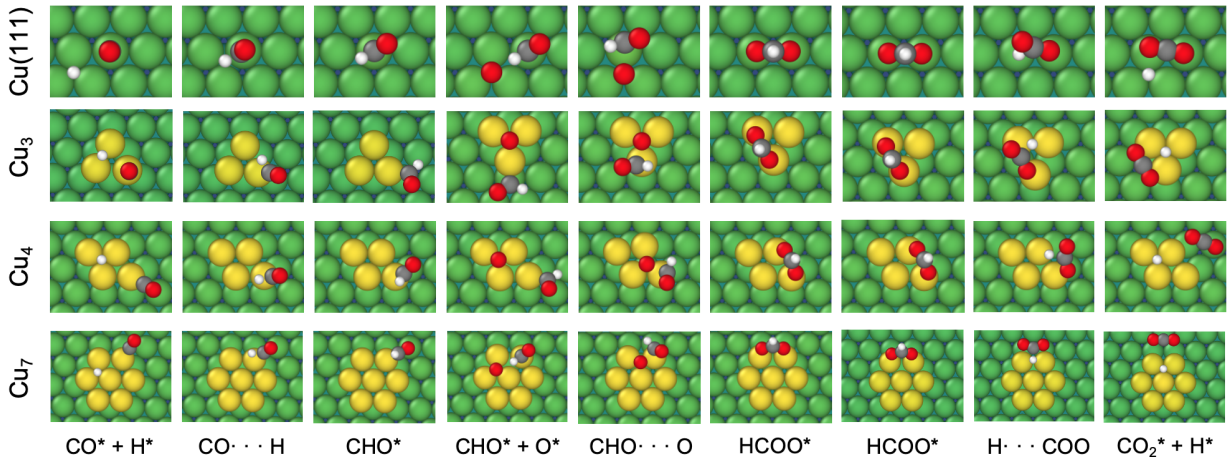

Figure S10: IS, TS, and FS of R7, R8, and R9 on Cu(111), Cu_3, Cu_4, and Cu_7

Figures S11 and S12 show the geometries of Cu_3 with CO coadsorption.

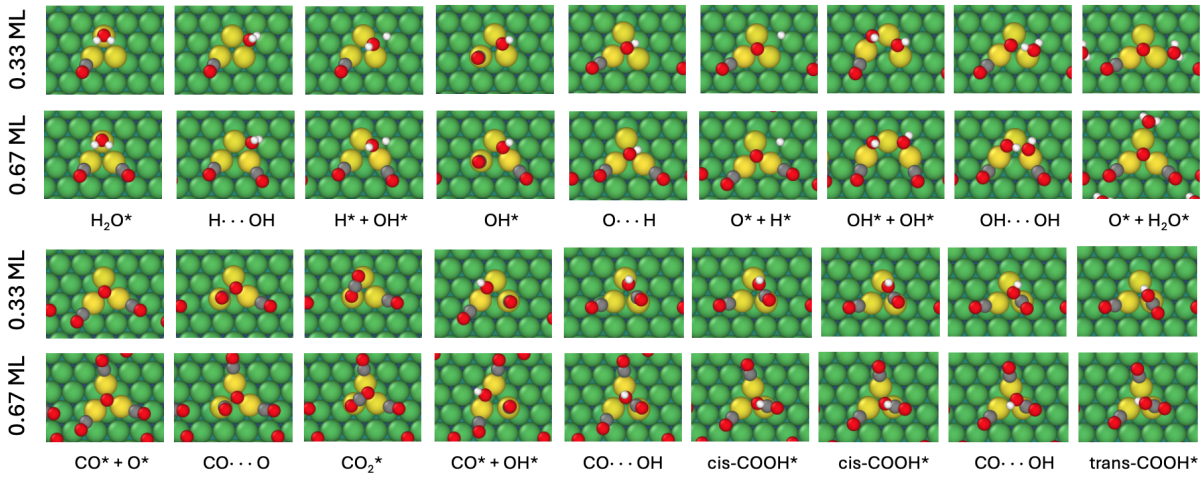

Figure S11: IS, TS, and FS of R2, R3, R3*, R4, R5, and R6a on Cu_3 with CO coadsorption

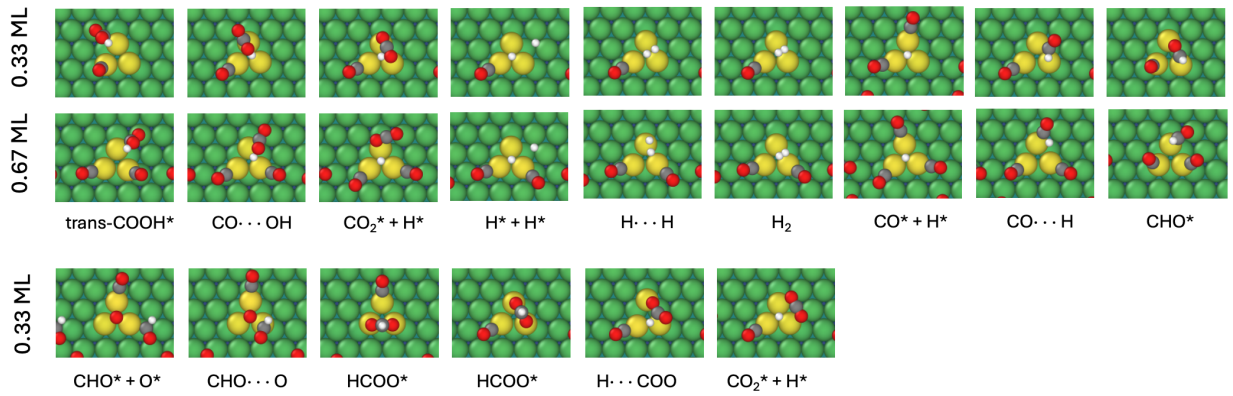

Figure S12: IS, TS, and FS of R6b, R6b*, R10, R7, R8, and R9 on Cu_3 with CO coadsorption

Figures S13 and S14 show the geometries of Cu_4 with CO coadsorption.

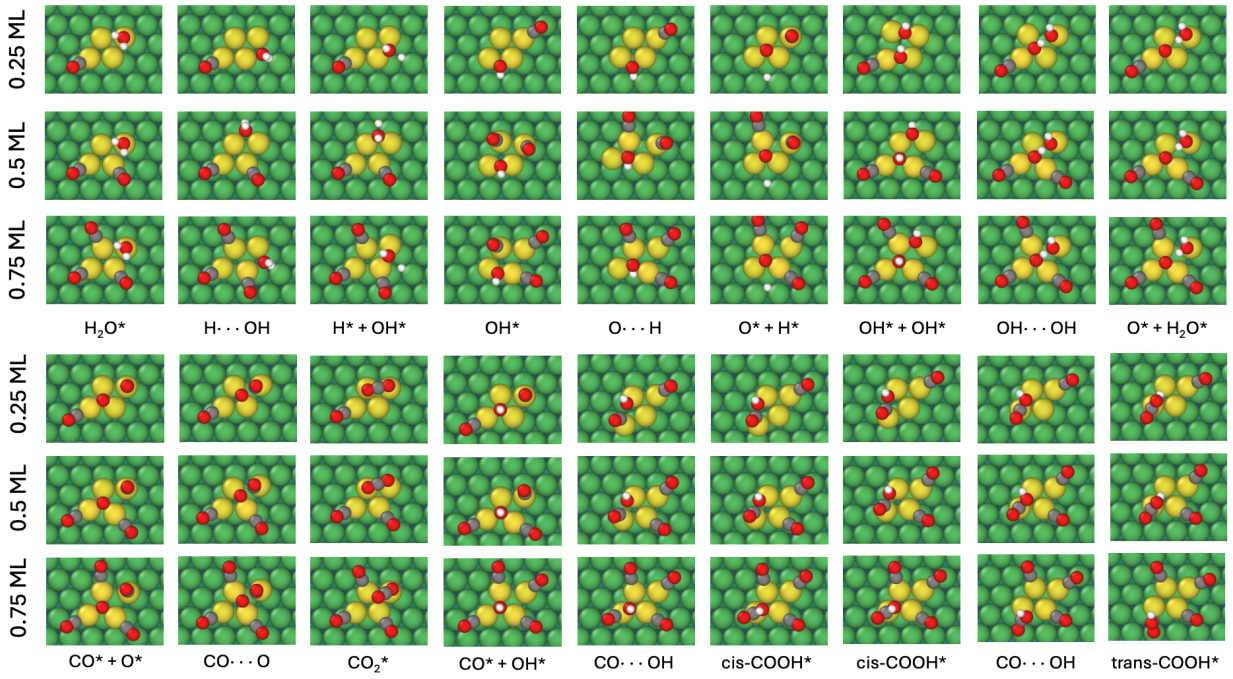

Figure S13: IS, TS, and FS of R2, R3, R3*, R4, R5, and R6a on Cu_4 with CO coadsorption

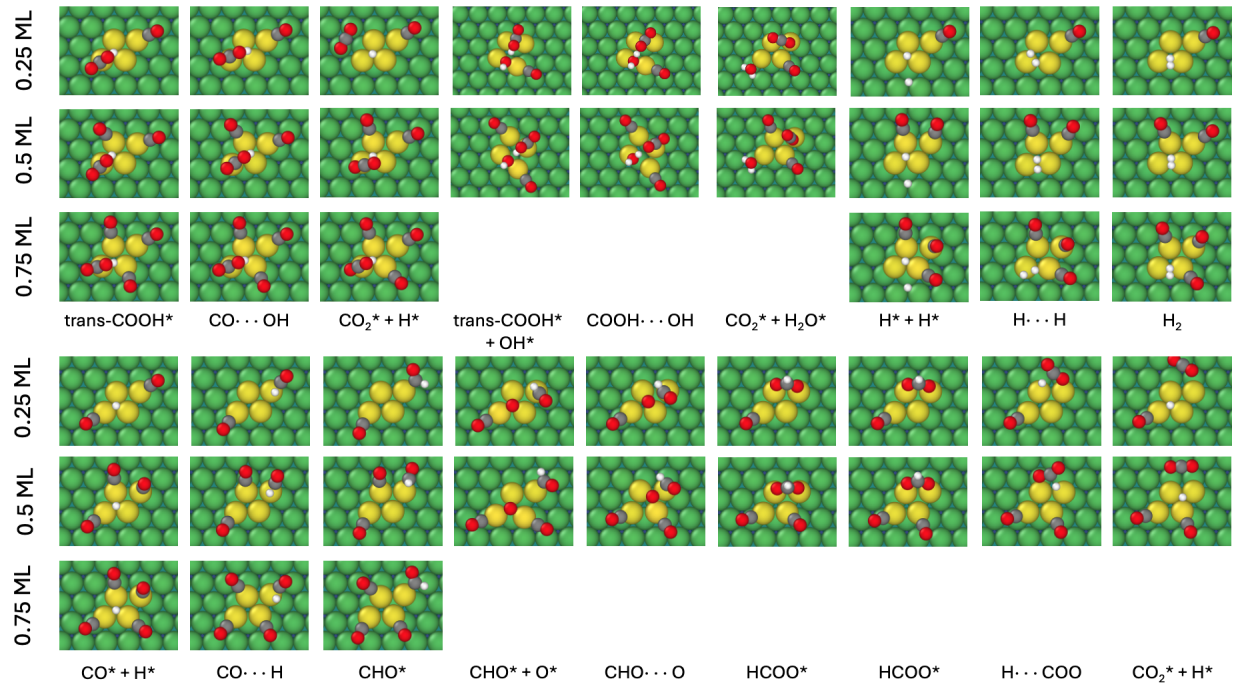

Figure S14: IS, TS, and FS of R6b, R6b*, R10, R7, R8, and R9 on Cu_4 with CO coadsorption

Figures S15–S18 show the geometries of Cu_7 with CO coadsorption.

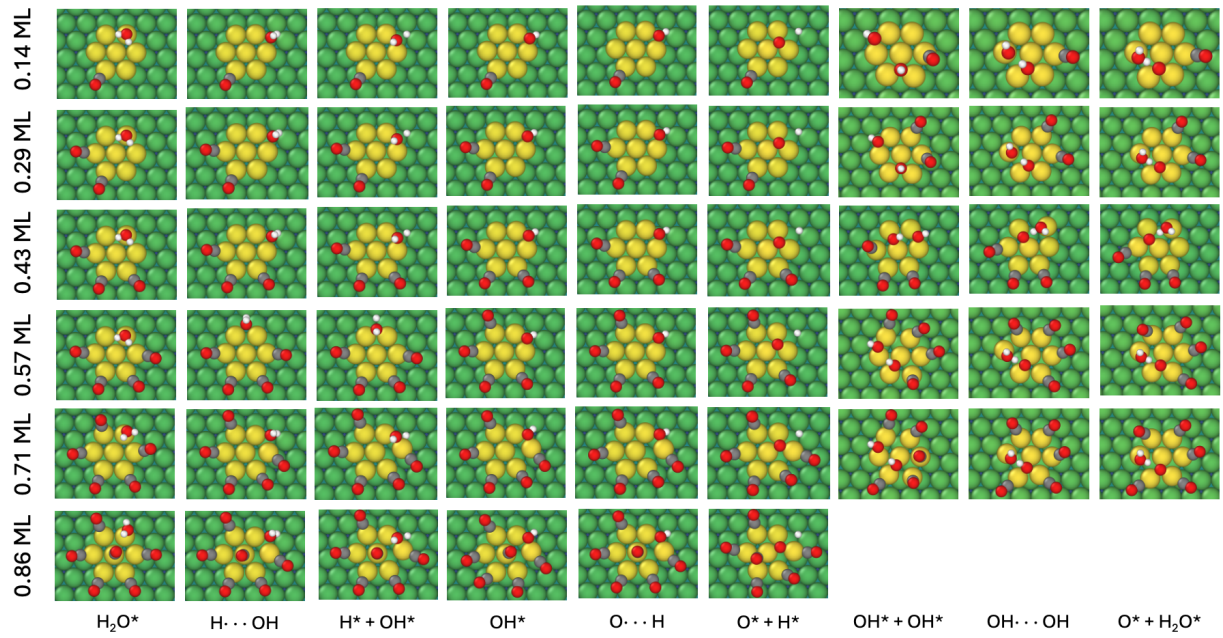

Figure S15: IS, TS, and FS of R2, R3, and R3* on Cu_7 with CO coadsorption

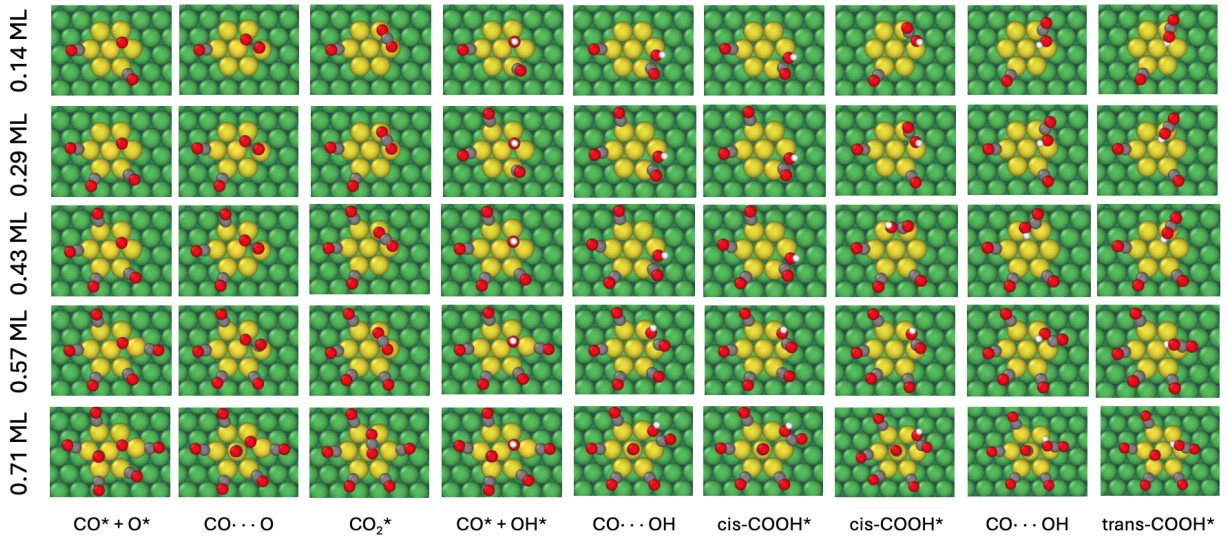

Figure S16: IS, TS, and FS of R4, R5, and R6a on Cu_7 with CO coadsorption

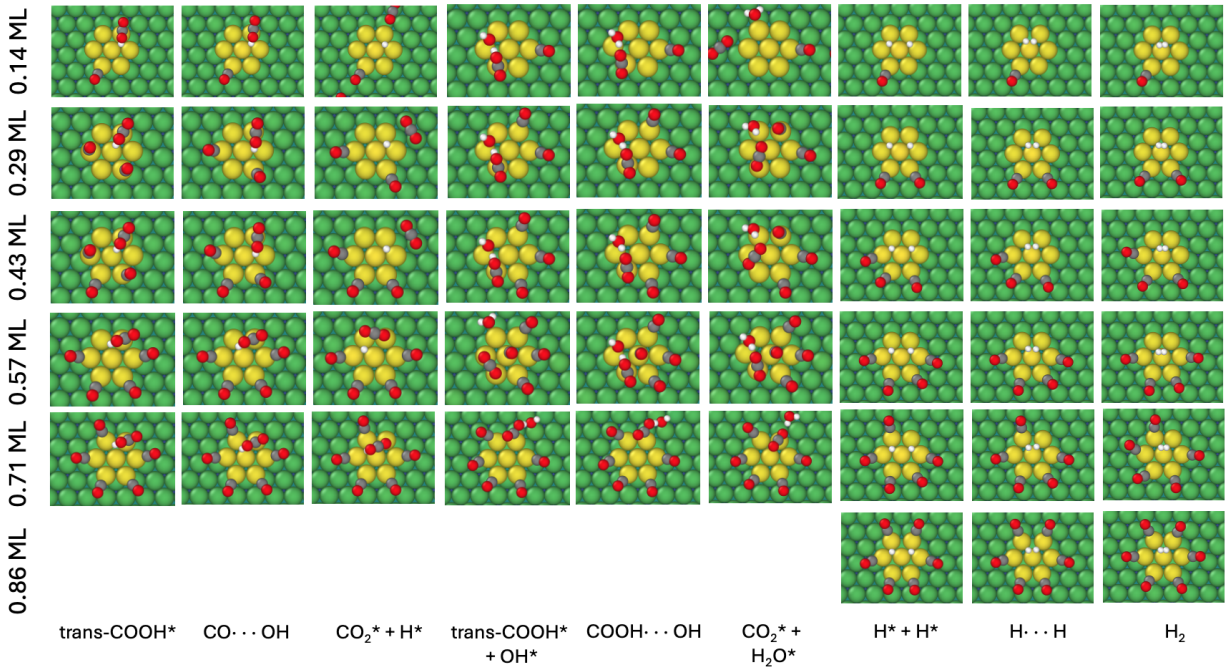

Figure S17: IS, TS, and FS of R6b, R6b*, and R10 on Cu_7 with CO coadsorption

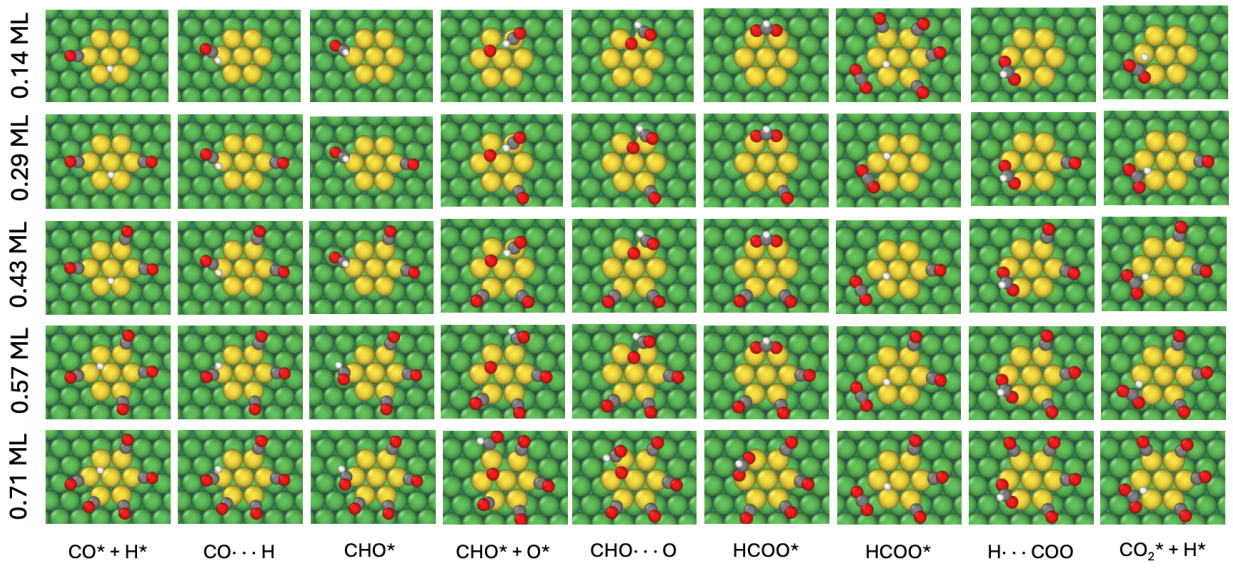

Figure S18: IS, TS, and FS of R7, R8, and R9 on Cu_7 with CO coadsorption

S5 Activation and Reaction Energy

The activation energy and reaction energy for each elementary step can be obtained from the Table S7, S9, S11, and S13 for Cu(111), Cu_7, Cu_4, and Cu_3, respectively. For example, if one want to know the activation energy of the water dissociation ($H_2O^* \rightarrow OH^* + H^*$) on Cu(111), look at Table S7, find the energy of H_2O at 0 CO coverage, which is -0.35 eV for the formation energy, and for the transition state (OH-H) which is 1.02 eV, therefore the activation energy is 1.37 eV.

S6 Microkinetic Modeling

The coverage-dependent microkinetic simulations were performed using the CatMAP package[11,12] following the work by Yang *et al.*[13] to describe the lateral adsorbate–adsorbate interactions using a second-order expansion in terms of coverage for the integral adsorption energy. CO* is anticipated to bond more strongly to Cu clusters than Cu(111), making it likely the predominant surface intermediate. Therefore, our model incorporates all surface

intermediate interactions with CO*. Cross-interaction parameters were derived from DFT calculations of adsorption energies at high CO* coverages. The model was solved by initially converging without interactions and then gradually increasing interaction strength by 0.025 until reaching 1.0.

Catalytic sites were defined as surface Cu atoms. Accordingly, the total number of sites N_{site} equals the number of surface Cu atoms in each model system: $N_{\text{site}} = 16$ for the Cu(111) slab unit cell employed in this work, and $N_{\text{site}} = 7$, 4, and 3 for the Cu_7, Cu_4, and Cu_3 clusters, respectively. Adsorbate coverages were normalized with respect to these site counts, such that adsorption of a single species corresponds to coverages of 1/16 on Cu(111) and 1/7, 1/4, and 1/3 on Cu_7, Cu_4, and Cu_3, respectively.

Within this mean-field framework, explicit differentiation of individual site types (e.g., corner, edge, or facet sites on clusters) was not introduced as separate site pools. Instead, for each adsorbed intermediate and elementary reaction step, representative adsorption geometries and free energies obtained from extensive MLFF sampling followed by DFT refinement were used to parameterize the microkinetic model. This treatment captures the intrinsic reactivity of each cluster size while maintaining a consistent and physically meaningful definition of surface coverage and turnover frequency across different catalyst models.

Turnover frequencies reported in this work are normalized per surface Cu-atom site as defined above; TOFs per cluster can be obtained by multiplying by N_{site} for the corresponding cluster size.

S6.1 Model Parametrization

The interaction model requires parameterization through three free parameters: the function f_{sq}, the interaction matrix ϵ_{ij}, and the reference adsorption energy E_i^0. Of these, E_i^0 corresponds to the differential adsorption energy at $\theta_i = 0$, typically obtained at low coverage ($\theta_i < 0.25$). The most flexible parameter is f_{sq}, which describes the coverage dependence of adsorption energy. While f_{sq} could in principle be arbitrarily complex, simple functional

forms such as piecewise-linear relations with a critical coverage cutoff are preferred to avoid overfitting. The matrix ϵ_{ij} quantifies pairwise adsorbate interactions and generally requires the most data; in this work, $\epsilon_{CO,i}$ values were obtained from a combination of low-coverage reference structures and selected high-coverage configurations. To efficiently generate these structures, we used our MLFF to sample the Cu clusters, while a combination of MLFF and minima hopping was used for Cu(111), followed by DFT single-point validation.

A smooth pairwise linear function is used for f_{sq}, with cutoffs specific to each surface. For Cu(111), the cutoff is 0.33; for Cu_7, 0.28; for Cu_4, 0.25; and for Cu_3, 0.33. The energy data used to fit the ϵ_{ij} parameters for Cu(111), Cu_7, Cu_4, and Cu_3 are shown in Tables S7, S9, S11, and S13, respectively. The resulting $\epsilon * ij$ parameters for Cu(111), Cu_7, Cu_4, and Cu_3 are presented in Tables S6, S8, S10, and S12, respectively.

S6.2 Free Energy Diagram

All free-energy diagrams are generated from the CatMAP output. The free-energy diagram without lateral interactions for Cu(111) and Cu clusters via the redox, carboxyl, and formate pathways is shown in Figure S19. The free-energy diagrams with and without lateral interactions via the redox and carboxyl pathways for all systems at 1 bar and 400, 450, and 550 K are shown in Figures S20, S21, and S22, respectively. The free-energy diagrams with and without lateral interactions via the OH-assisted redox and carboxyl-hydroxyl pathways for all systems at 1 bar and 450 and 500 K are shown in Figures S23 and S24, respectively.

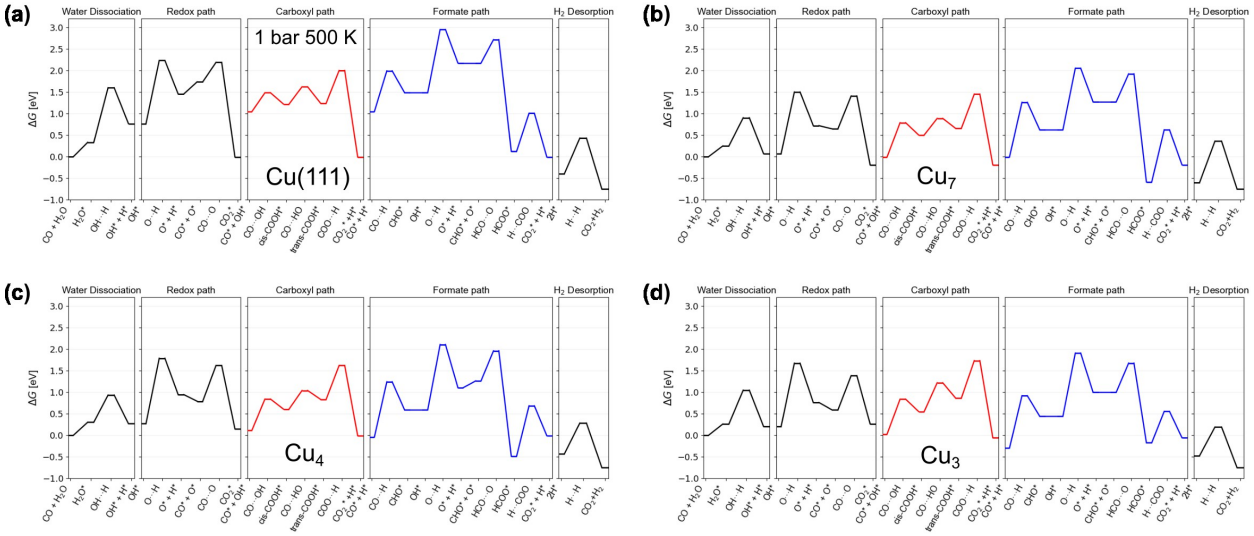

Figure S19: Free energy diagrams of the WGSR on (a) Cu(111), (b) Cu_7, (c) Cu_4, and (d) Cu_3 at 500 K and 1 bar, calculated without lateral interaction. The reference is CO and H_2O in gas phase.

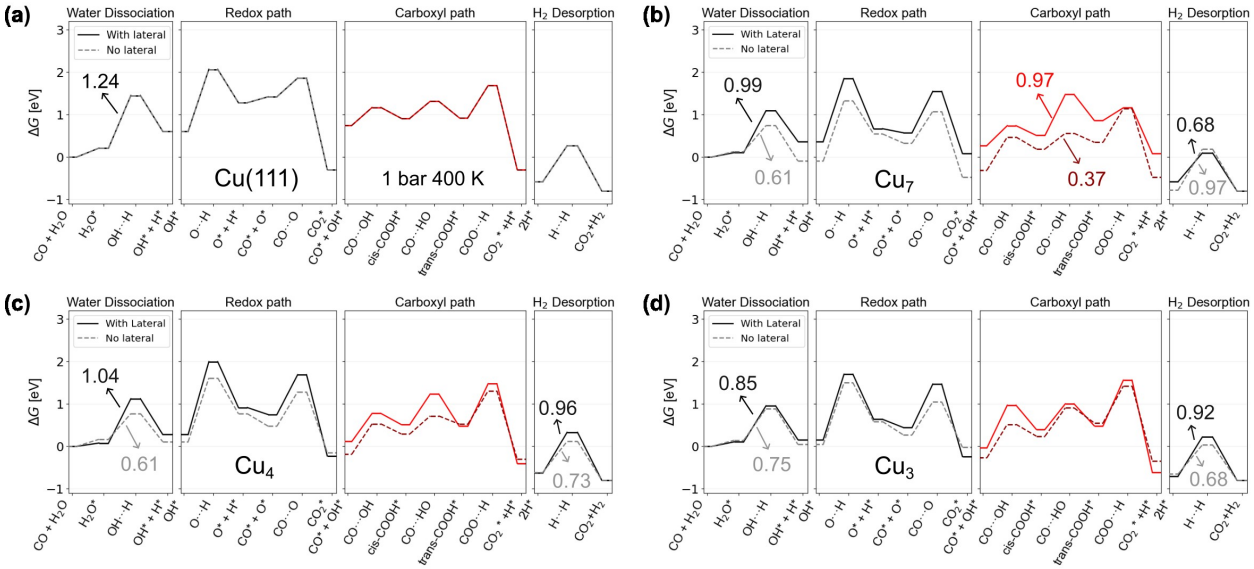

Figure S20: Free energy diagrams of the WGSR via redox and carboxyl pathways at 400 K and 1 bar on (a) Cu(111), (b) Cu_7, (c) Cu_4, and (d) Cu_3, shown with (solid lines) and without (dashed lines) lateral interaction. The reference is CO and H_2O in gas phase.

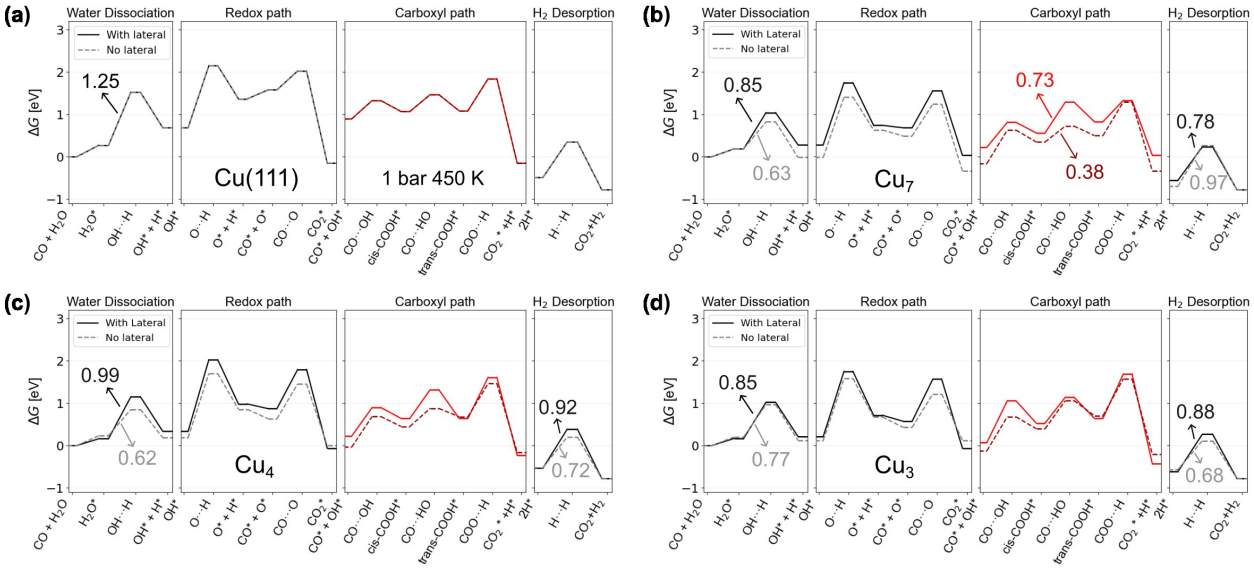

Figure S21: Free energy diagrams of the WGSR via redox and carboxyl pathways at 450 K and 1 bar on (a) Cu(111), (b) Cu_7, (c) Cu_4, and (d) Cu_3, shown with (solid lines) and without (dashed lines) lateral interaction. The reference is CO and H_2O in gas phase.

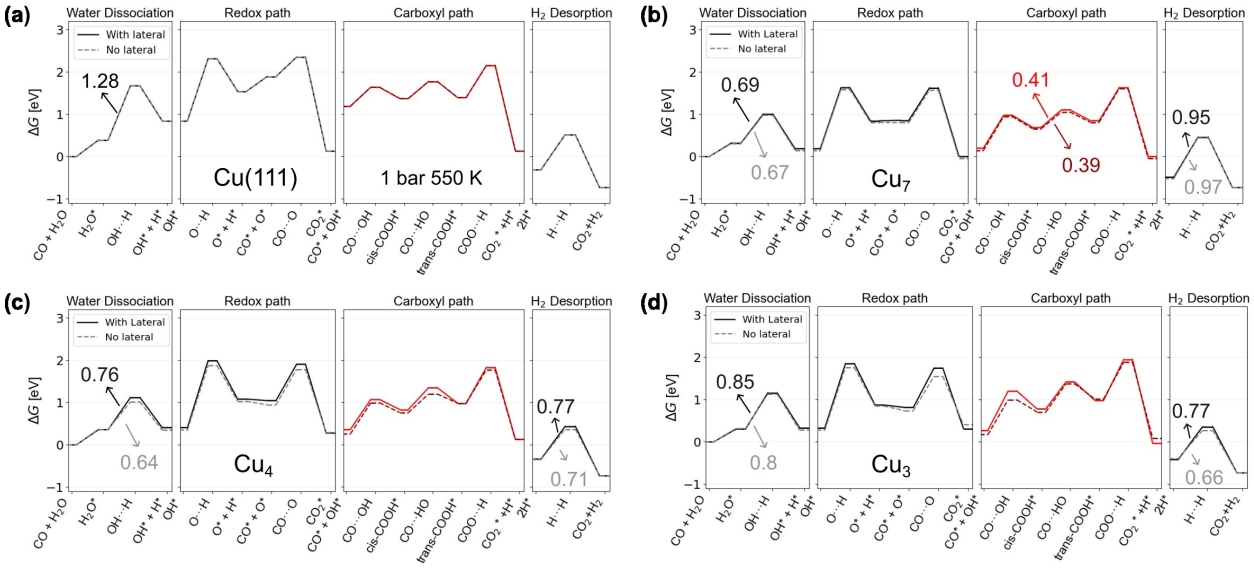

Figure S22: Free energy diagrams of the WGSR via redox and carboxyl pathways at 550 K and 1 bar on (a) Cu(111), (b) Cu_7, (c) Cu_4, and (d) Cu_3, shown with (solid lines) and without (dashed lines) lateral interaction. The reference is CO and H_2O in gas phase.

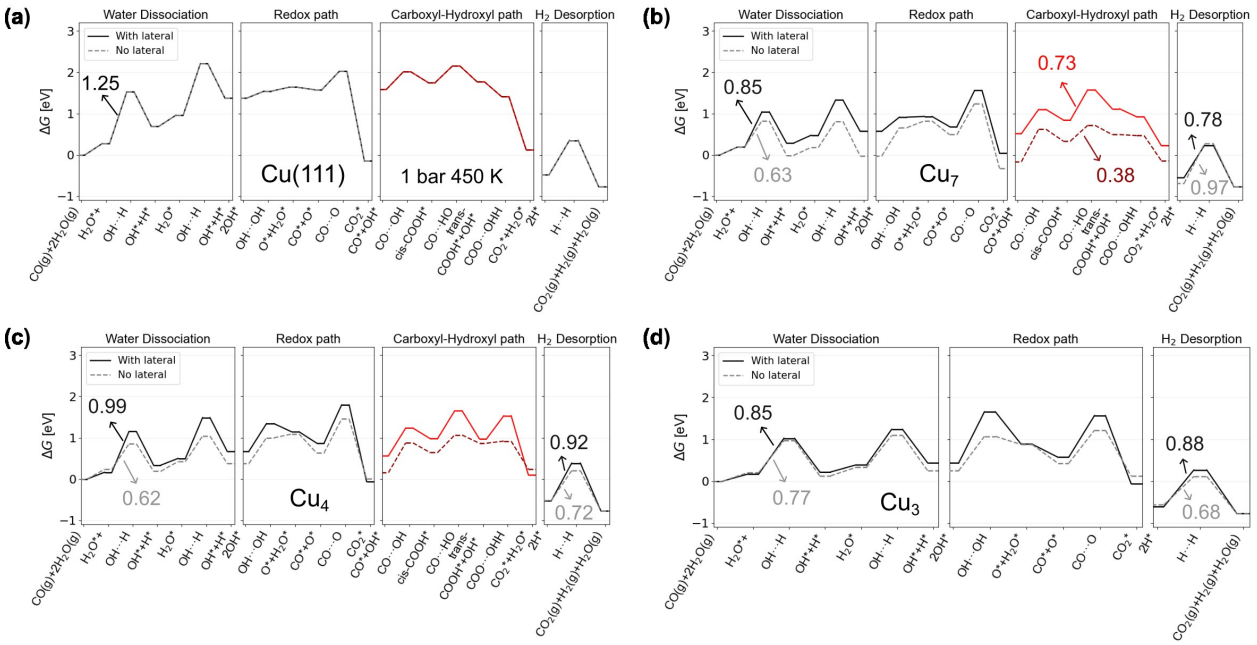

Figure S23: Free energy diagrams of the WGSR via OH-assisted redox and carboxyl-hydroxyl pathways at 450 K and 1 bar on (a) Cu(111), (b) Cu_7, (c) Cu_4, and (d) Cu_3, shown with (solid lines) and without (dashed lines) lateral interaction. The reference is CO and $2H_2O$ in gas phase.

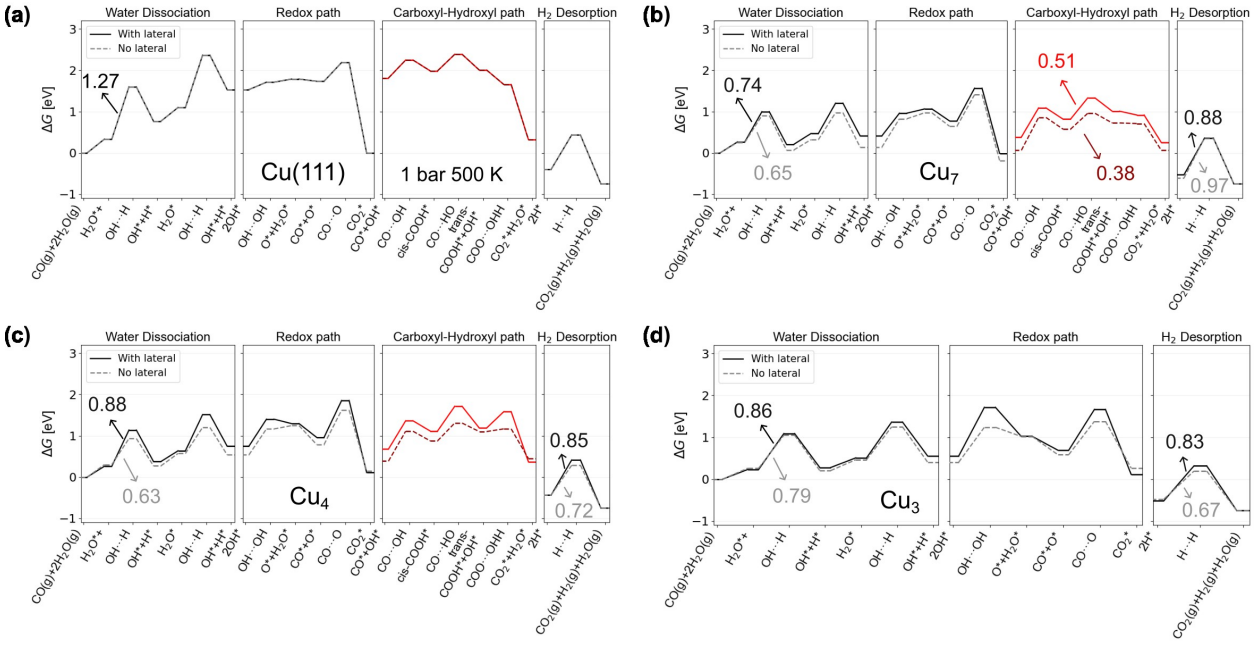

Figure S24: Free energy diagrams of the WGSR via OH-assisted redox and carboxyl-hydroxyl pathways at 500 K and 1 bar on (a) Cu(111), (b) Cu_7, (c) Cu_4, and (d) Cu_3, shown with (solid lines) and without (dashed lines) lateral interaction. The reference is CO and $2H_2O$ in gas phase.

S6.3 Microkinetic Results

The TOF dependence on total pressure and on the CO:H_2O partial pressure ratio is shown in Figures S25 and S26, respectively. The TOF under the exact experimental conditions reported by Campbell *et al.*[14] is shown in Figure S27. To clearly illustrate the effect of including lateral interactions at 1 bar and a 1:1 CO:H_2O ratio, see Figure S28.

The steady-state coverages of all species without and with lateral interactions at 1 bar and a 1:1 CO:H_2O ratio are shown in Figures S29 and S30, respectively. The DRC plot without lateral interactions (1 bar, 1:1 CO:H_2O) is shown in Figure S31. The dominant pathway without lateral interactions (1 bar, 1:1 CO:H_2O) is shown in Figure S32. The reaction orders without and with lateral interactions (1 bar, 1:1 CO:H_2O) are shown in Figures S33 and S34, respectively. The Arrhennius plot is shown in FiguresS35 and S36 for the case without and with the lateral interaction at 1 bar and 1:1 CO:H_2O.

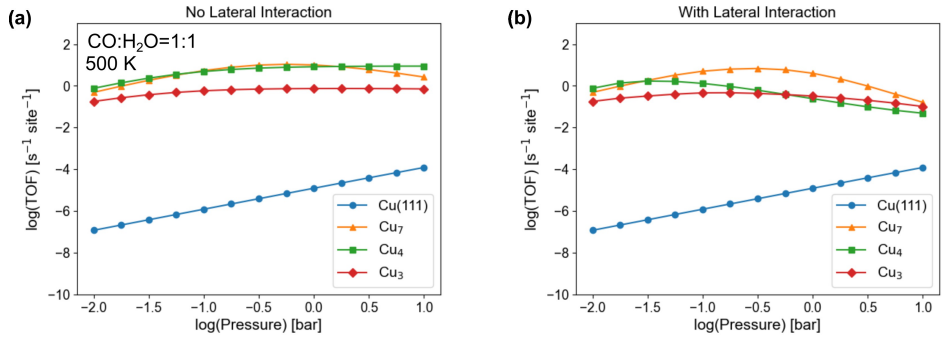

Figure S25: TOF vs log Pressure on Cu clusters and Cu(111) at 500 K (a) without and (b) with lateral interaction.

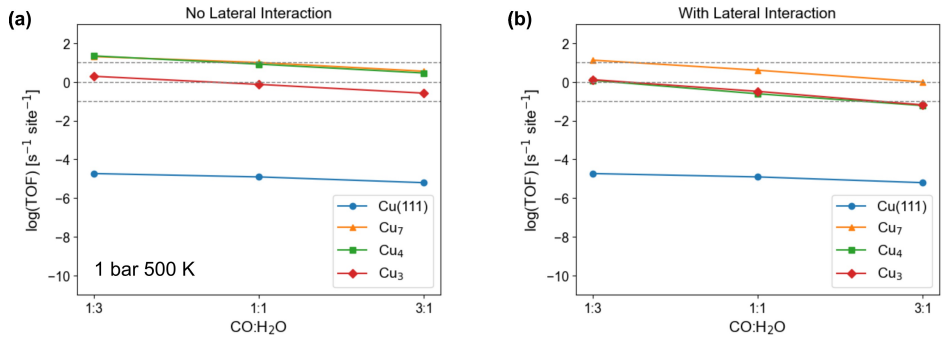

Figure S26: TOF vs CO:H_2O partial pressure ratio on Cu clusters and Cu(111) at 500 K 1 bar (a) without and (b) with lateral interaction.

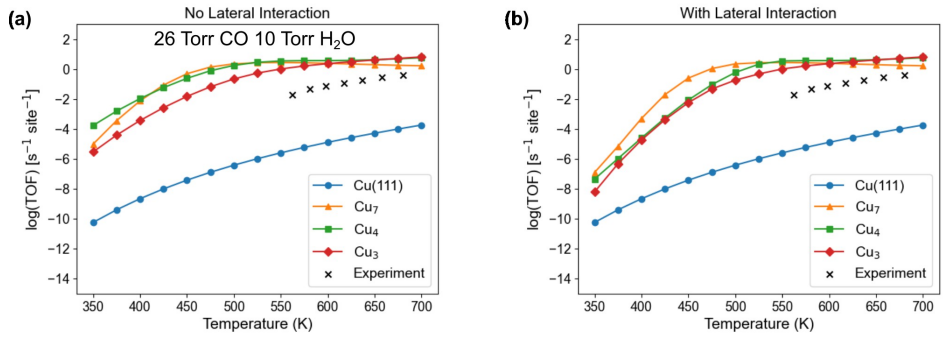

Figure S27: TOF vs temperature on Cu clusters and Cu(111) at with 26 Torr CO and 10 Torr H_2O following the experiment by Campbell[14] (a) without and (b) with lateral interaction.

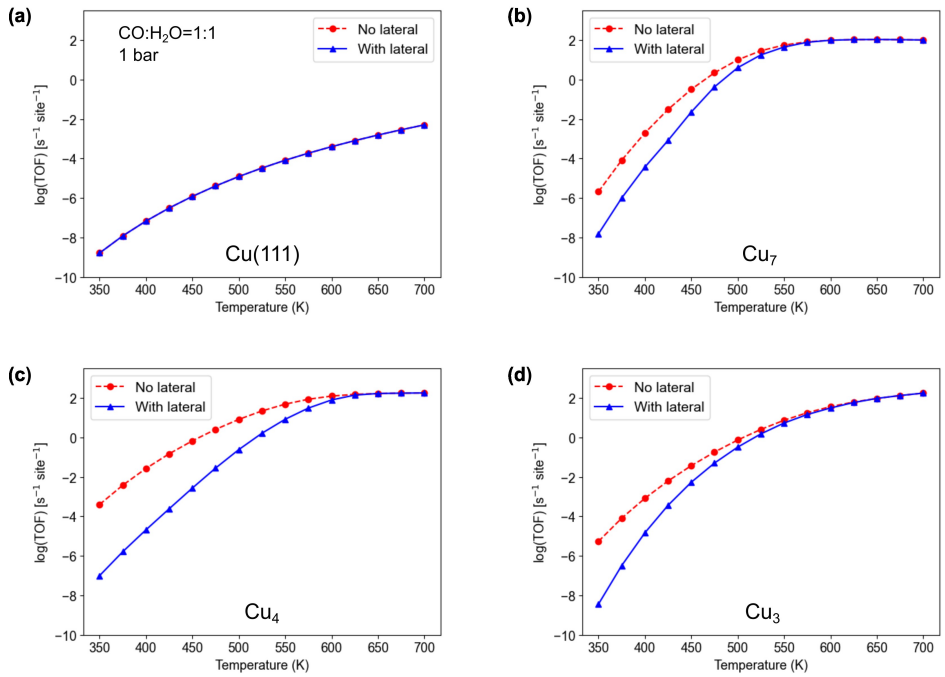

Figure S28: TOF vs temperature on (a) Cu(111), (b) Cu_3/Cu(111), (c) Cu_4/Cu(111), and (d) Cu_7/Cu(111) at 1 bar with (blue triangles) and without (red dashed circles) lateral interaction.

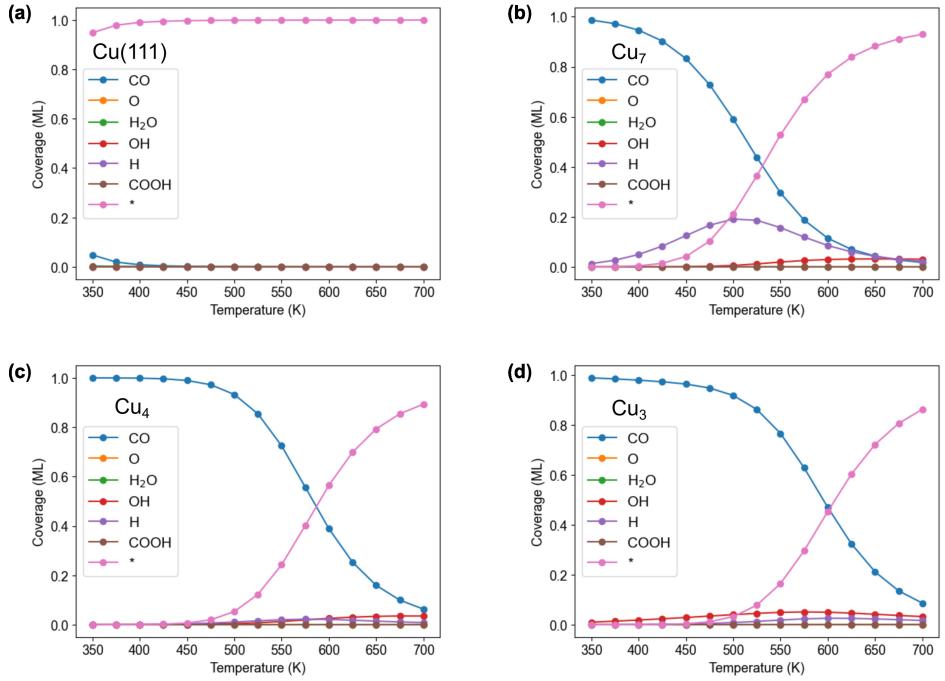

Figure S29: Steady state coverage vs temperature of each species on (a) Cu(111), (b) Cu_3/Cu(111), (c) Cu_4/Cu(111), and (d) Cu_7/Cu(111) at 1 bar without lateral interaction.

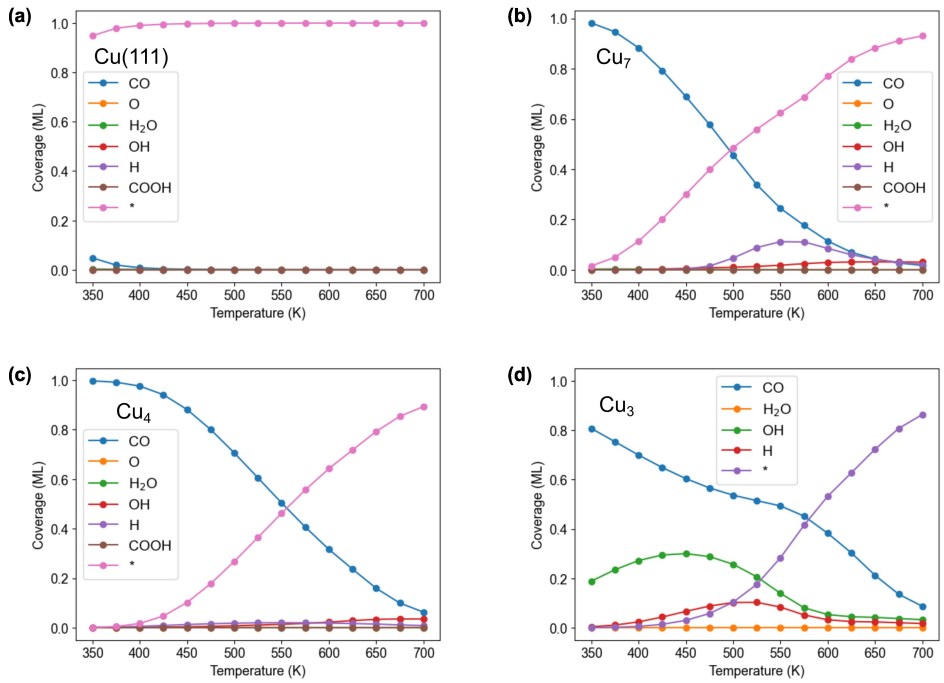

Figure S30: Steady state coverage vs temperature of each species on (a) Cu(111), (b) Cu_3/Cu(111), (c) Cu_4/Cu(111), and (d) Cu_7/Cu(111) at 1 bar with lateral interaction.

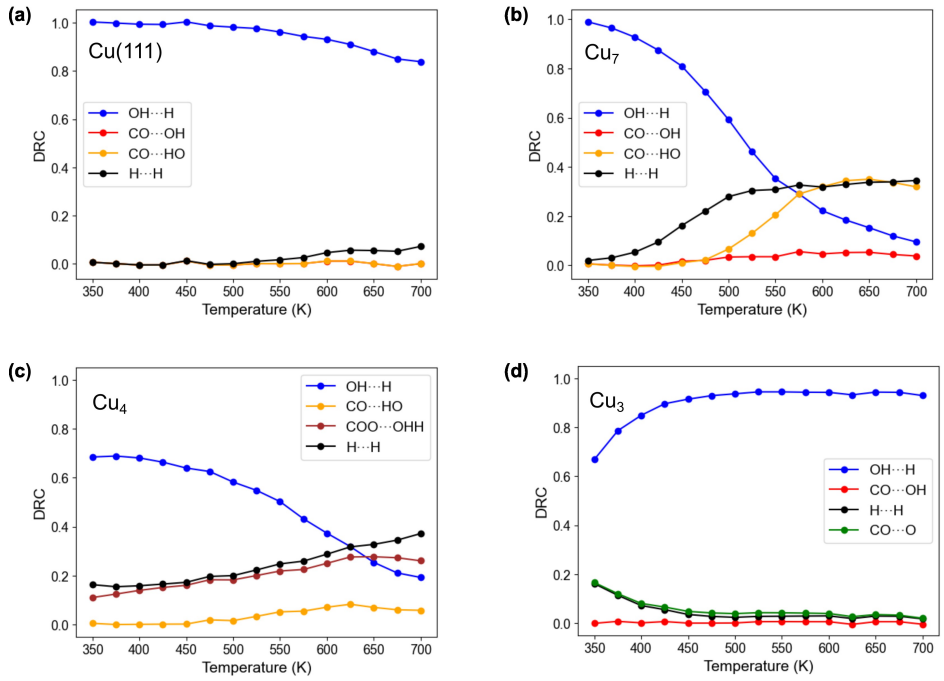

Figure S31: DRC on (a) Cu(111), (b) Cu_3/Cu(111), (c) Cu_4/Cu(111), and (d) Cu_7/Cu(111) at 1 bar without lateral interaction.

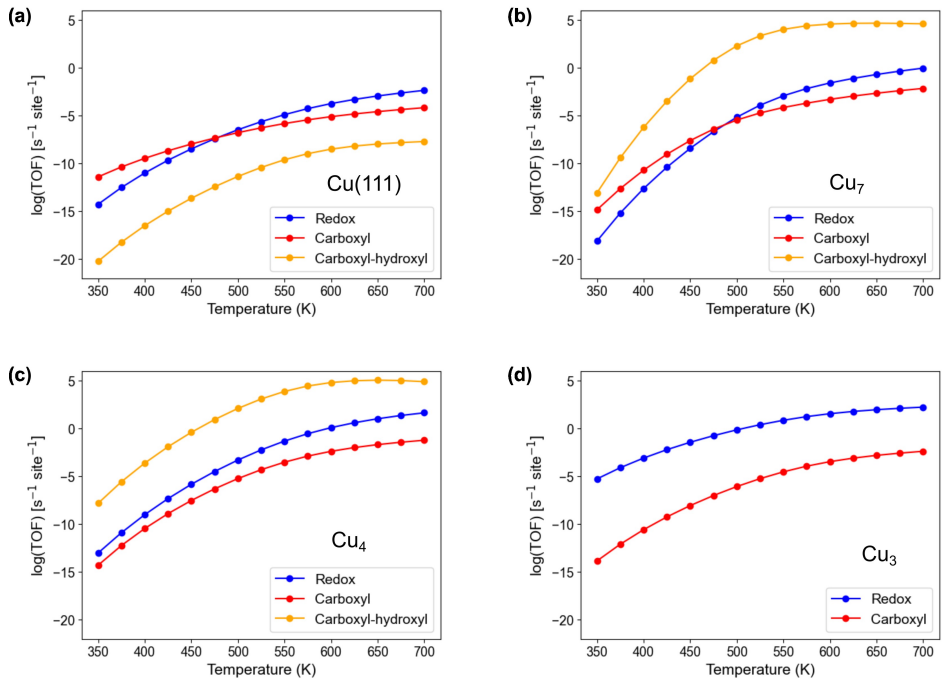

Figure S32: Dominant pathways on (a) Cu(111), (b) Cu_3/Cu(111), (c) Cu_4/Cu(111), and (d) Cu_7/Cu(111) at 1 bar without lateral interaction.

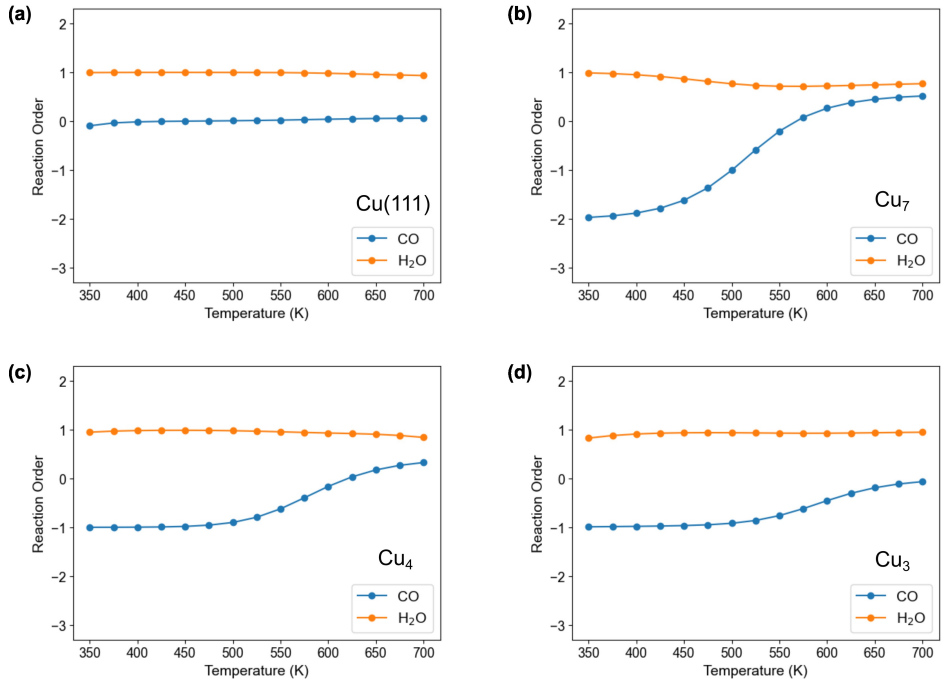

Figure S33: Reaction order vs temperatures on (a) Cu(111), (b) Cu_3/Cu(111), (c) Cu_4/Cu(111), and (d) Cu_7/Cu(111) at 1 bar without lateral interaction.

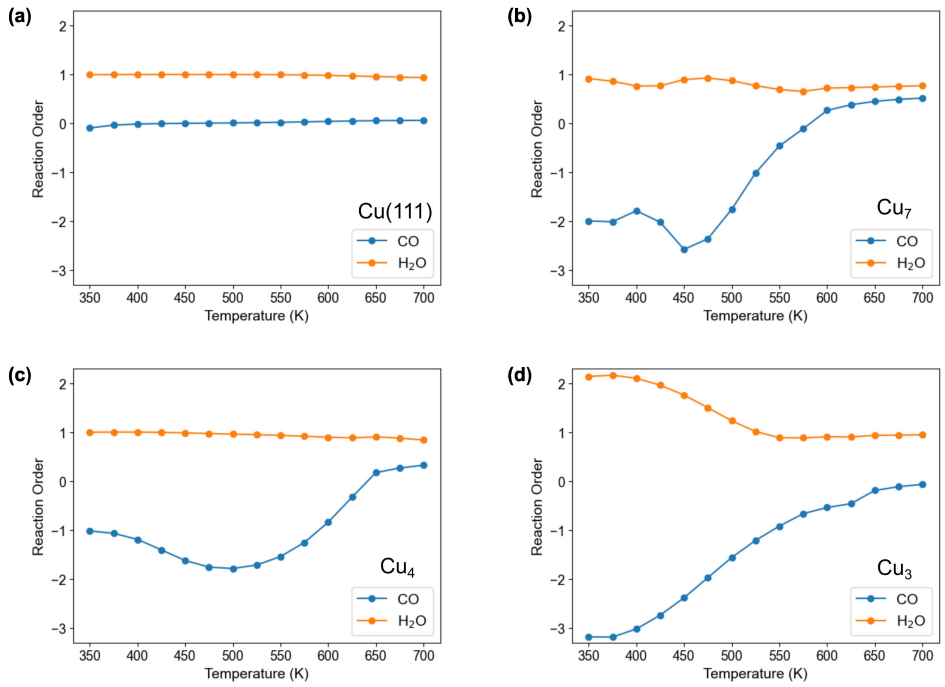

Figure S34: Reaction order vs temperatures on (a) Cu(111), (b) Cu_3/Cu(111), (c) Cu_4/Cu(111), and (d) Cu_7/Cu(111) at 1 bar with lateral interaction.

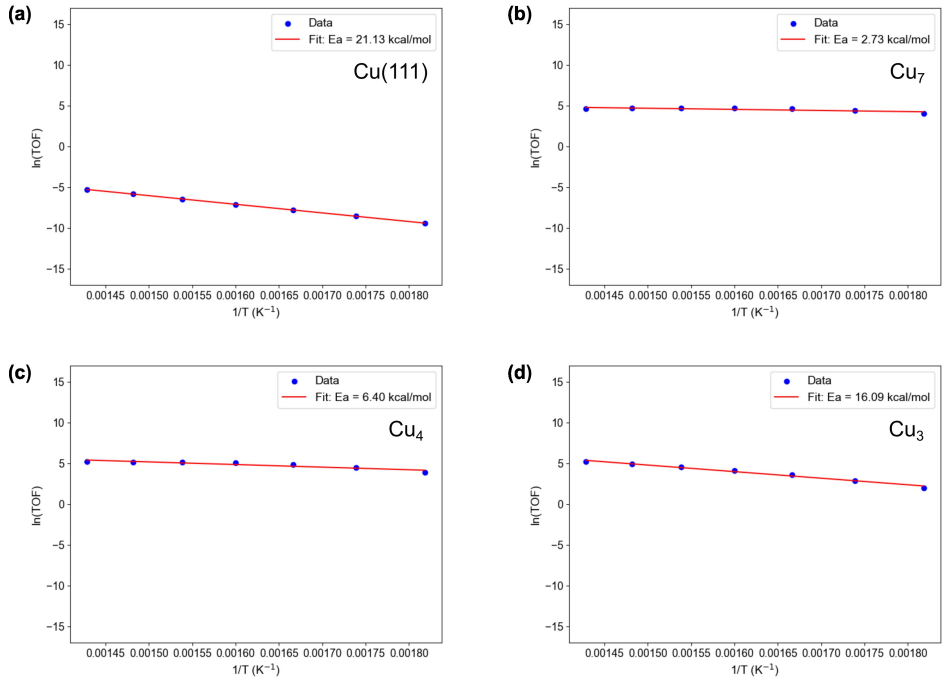

Figure S35: Arrhennius plot on (a) Cu(111), (b) Cu_3/Cu(111), (c) Cu_4/Cu(111), and (d) Cu_7/Cu(111) at 1 bar without lateral interaction.

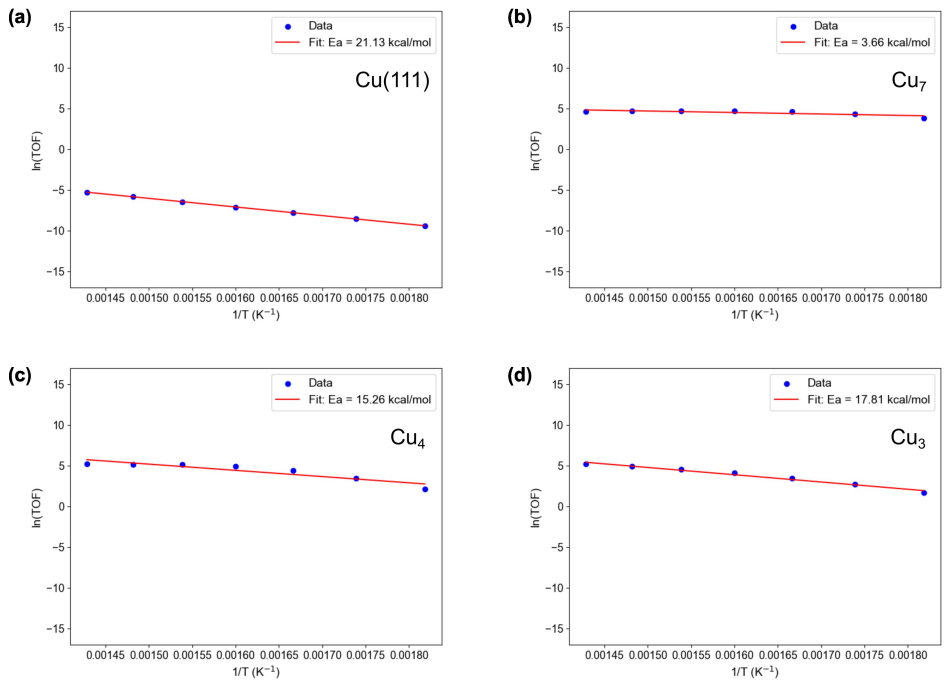

Figure S36: Arrhennius plot on (a) Cu(111), (b) Cu_3/Cu(111), (c) Cu_4/Cu(111), and (d) Cu_7/Cu(111) at 1 bar with lateral interaction.

S6.4 Effect of cluster size distribution on the overall TOF

Under realistic experimental conditions, supported Cu catalysts are expected to exhibit a distribution of cluster sizes rather than a single, uniform cluster type. In such cases, the overall catalytic activity can be expressed as a weighted combination of the intrinsic activities of individual cluster sizes.

When TOFs are expressed on a per-cluster basis, the overall cluster-normalized TOF is given by

$$\mathrm{TOF}_{\mathrm{overall}}^{(\mathrm{cluster})} = \sum_i f_i^{(\mathrm{cluster})}\, \mathrm{TOF}_i^{(\mathrm{cluster})}, \tag{1}$$

where $\mathrm{TOF}_i^{(\mathrm{cluster})} = N_{\mathrm{site},i}\, \mathrm{TOF}_i^{(\mathrm{site})}$, with $N_{\mathrm{site},i}$ being the number of surface Cu atoms for cluster size i, and $f_i^{(\mathrm{cluster})}$ is the number fraction of clusters of a given cluster size i in the catalyst.

In the present work, the microkinetic simulations focus on the intrinsic reactivity of

individual, well-defined cluster sizes in order to elucidate structure–activity relationships and the impact of CO coadsorption. Incorporation of experimentally determined cluster size distributions into an ensemble-averaged kinetic model can be readily achieved using the expressions above and represents a natural extension of the present framework when such distributions are available.

S6.5 Cu(111) Elementary Steps

These are the elementary steps used in the microkinetic modeling for Cu(111) surface.

$$*_s + CO_{(g)} \leftrightarrow CO^{*_s} \tag{2}$$

$$*_s + H_2O_{(g)} \leftrightarrow H_2O^{*_s} \tag{3}$$

$$CO_{2(g)} + *_s \leftrightarrow CO_2^{*_s} \tag{4}$$

$$H_2O^{*_s} + *_s \leftrightarrow OH{-}H^{*_s} + *_s \rightarrow H^{*_s} + OH^{*_s} \tag{5}$$

$$OH^{*_s} + *_s \leftrightarrow O{-}H^{*_s} + *_s \rightarrow O^{*_s} + H^{*_s} \tag{6}$$

$$OH^{*_s} + OH^{*_s} \leftrightarrow O{-}OHH^{*_s} + *_s \rightarrow H_2O^{*_s} + O^{*_s} \tag{7}$$

$$CO^{*_s} + O^{*_s} \leftrightarrow CO{-}O^{*_s} + *_s \rightarrow CO_2^{*_s} + *_s \tag{8}$$

$$CO^{*_s} + OH^{*_s} \leftrightarrow CO{-}OH^{*_s} + *_s \rightarrow COOH^{*_s} + *_s \tag{9}$$

$$COOH^{*_s} \leftrightarrow CO{-}HO^{*_s} \rightarrow COHO^{*_s} \tag{10}$$

$$COHO^{*_s} + *_s \leftrightarrow COO{-}H^{*_s} + *_s \rightarrow CO_2^{*_s} + H^{*_s} \tag{11}$$

$$COHO^{*_s} + OH^{*_s} \leftrightarrow COO{-}OHH^{*_s} + *_s \rightarrow CO_2^{*_s} + H_2O^{*_s} \tag{12}$$

$$H^{*_s} + H^{*_s} \leftrightarrow H{-}H^{*_s} + *_s \rightarrow H_{2(g)} + *_s + *_s \tag{13}$$

S6.6 Cu(111) Interaction Parameters

All unlisted $\epsilon_{i,j}$ in Table S6 are assumed to be zero.

Table S6: Lateral interaction parameters $\epsilon_{i,j}$ on Cu(111).

i	j	$\epsilon_{i,j}$
CO	CO	1.52
CO	CO_2	6.28
CO	COHO	6.10
CO	COOH	7.63
CO	H_2O	1.93
CO	H	1.50
CO	OH	2.65
CO	O	8.06
CO	CO-HO	1.87
CO	CO-OH	2.14
CO	CO-O	5.85
CO	COO-H	14.79
CO	COO-OHH	32.02
CO	H-H	-1.61
CO	O-H	5.12
CO	O-OHH	3.96
CO	OH-H	0.70

S6.7 Cu(111) Energies and Frequencies

Table S7 summarizes the adsorbates, coadsorbates, their coverages, integral formation energies (E_{int}), formation energies, and vibrational frequencies on Cu(111).

Table S7: Adsorbates, coadsorbates, formation energies, and frequencies for Cu(111).

Adsorbate	Coverage	Coadsorbate	Coadsorbate coverage	$E_{int}(\theta_i)[eV]$	Formation energy [eV]	Frequencies [cm^{-1}]
CO(g)	0.00	None	0.00	0.00	0.00	2165.5
CO2(g)	0.00	None	0.00	-0.84	-0.84	2401.6, 1328.9, 642.0, 642.0
H2(g)	0.00	None	0.00	0.00	0.00	4403.9
H2O(g)	0.00	None	0.00	0.00	0.00	3898.9, 3794.3, 1580.8
CO	0.06	None	0.00	-0.03	-0.48	2052.3, 316.9, 280.6, 280.6, 50.0, 50.0
CO	0.12	None	0.00	-0.06	-0.47	2052.3, 316.9, 280.6, 280.6, 50.0, 50.0
CO	0.19	None	0.00	-0.09	-0.42	2052.3, 316.9, 280.6, 280.6, 50.0, 50.0
CO	0.25	None	0.00	-0.12	-0.50	2052.3, 316.9, 280.6, 280.6, 50.0, 50.0
CO	0.31	None	0.00	-0.14	-0.40	2052.3, 316.9, 280.6, 280.6, 50.0, 50.0
CO	0.38	None	0.00	-0.17	-0.48	2052.3, 316.9, 280.6, 280.6, 50.0, 50.0
CO	0.44	None	0.00	-0.19	-0.36	2052.3, 316.9, 280.6, 280.6, 50.0, 50.0
CO	0.50	None	0.00	-0.21	-0.19	2052.3, 316.9, 280.6, 280.6, 50.0, 50.0
CO	0.56	None	0.00	-0.22	-0.31	2052.3, 316.9, 280.6, 280.6, 50.0, 50.0
H2O	0.06	None	0.00	-0.02	-0.35	3750.4, 3669.2, 1556.8, 534.7, 470.5, 133.5, 124.2, 75.4, 50.0

Adsorbate	Coverage	Coadsorbate	Coadsorbate coverage	$E_{int}(\theta_i)[eV]$	Formation energy [eV]	Frequencies [cm^{-1}]
H2O	0.06	CO	0.06	-0.05	-0.36	3750.4, 3669.2, 1556.8, 534.7, 470.5, 133.5, 124.2, 75.4, 50.0
H2O	0.06	CO	0.12	-0.08	-0.39	3750.4, 3669.2, 1556.8, 534.7, 470.5, 133.5, 124.2, 75.4, 50.0
H2O	0.06	CO	0.25	-0.14	-0.37	3750.4, 3669.2, 1556.8, 534.7, 470.5, 133.5, 124.2, 75.4, 50.0
H2O	0.06	CO	0.62	-0.15	0.19	3750.4, 3669.2, 1556.8, 534.7, 470.5, 133.5, 124.2, 75.4, 50.0
OH	0.06	None	0.00	0.01	0.20	3823.2, 452.2, 446.8, 367.4, 225.5, 218.7
OH	0.06	CO	0.06	-0.02	0.18	3823.2, 452.2, 446.8, 367.4, 225.5, 218.7
OH	0.06	CO	0.12	-0.05	0.13	3823.2, 452.2, 446.8, 367.4, 225.5, 218.7
OH	0.06	CO	0.25	-0.11	0.14	3823.2, 452.2, 446.8, 367.4, 225.5, 218.7
OH	0.06	CO	0.62	-0.09	1.11	3823.2, 452.2, 446.8, 367.4, 225.5, 218.7
OH	0.06	CO	0.69	-0.01	1.02	3823.2, 452.2, 446.8, 367.4, 225.5, 218.7
O	0.06	None	0.00	0.07	1.09	447.3, 352.5, 352.3
O	0.06	CO	0.06	0.04	1.07	447.3, 352.5, 352.3
O	0.06	CO	0.12	0.00	1.00	447.3, 352.5, 352.3

Adsorbate	Coverage	Coadsorbate	Coadsorbate coverage	$E_{int}(\theta_i)[eV]$	Formation energy [eV]	Frequencies [cm^{-1}]
O	0.06	CO	0.56	-0.06	2.59	447.3, 352.5, 352.3
O	0.06	CO	0.62	0.00	2.63	447.3, 352.5, 352.3
COOH	0.06	None	0.00	-0.01	-0.17	3577.0, 1663.7, 1212.8, 955.6, 632.2, 623.1, 374.9, 246.1, 195.7, 54.7, 50.0, 50.0
COOH	0.06	CO	0.06	-0.04	-0.19	3577.0, 1663.7, 1212.8, 955.6, 632.2, 623.1, 374.9, 246.1, 195.7, 54.7, 50.0, 50.0
COOH	0.06	CO	0.12	-0.08	-0.25	3577.0, 1663.7, 1212.8, 955.6, 632.2, 623.1, 374.9, 246.1, 195.7, 54.7, 50.0, 50.0
COOH	0.06	CO	0.25	-0.14	-0.33	3577.0, 1663.7, 1212.8, 955.6, 632.2, 623.1, 374.9, 246.1, 195.7, 54.7, 50.0, 50.0
COOH	0.06	CO	0.56	-0.12	1.61	3577.0, 1663.7, 1212.8, 955.6, 632.2, 623.1, 374.9, 246.1, 195.7, 54.7, 50.0, 50.0
COOH	0.06	CO	0.62	-0.08	1.30	3577.0, 1663.7, 1212.8, 955.6, 632.2, 623.1, 374.9, 246.1, 195.7, 54.7, 50.0, 50.0
COHO	0.06	None	0.00	-0.01	-0.19	3606.7, 1671.1, 1232.5, 1024.9, 651.3, 600.1, 407.2, 255.8, 214.7, 67.4, 67.2, 50.0

Adsorbate	Coverage	Coadsorbate	Coadsorbate coverage	$E_{int}(\theta_i)[eV]$	Formation energy [eV]	Frequencies [cm^{-1}]
COHO	0.06	CO	0.50	-0.18	0.50	3606.7, 1671.1, 1232.5, 1024.9, 651.3, 600.1, 407.2, 255.8, 214.7, 67.4, 67.2, 50.0
COHO	0.06	CO	0.56	-0.18	0.75	3606.7, 1671.1, 1232.5, 1024.9, 651.3, 600.1, 407.2, 255.8, 214.7, 67.4, 67.2, 50.0
CHO	0.06	None	0.00	-0.01	-0.21	2792.1, 1674.1, 1132.1, 655.2, 400.7, 199.3, 57.7, 52.2, 50.0
CHO	0.06	CO	0.38	-0.20	-0.41	2792.1, 1674.1, 1132.1, 655.2, 400.7, 199.3, 57.7, 52.2, 50.0
CHO	0.06	CO	0.44	-0.21	-0.39	2792.1, 1674.1, 1132.1, 655.2, 400.7, 199.3, 57.7, 52.2, 50.0
CHO	0.06	CO	0.50	-0.22	-0.18	2792.1, 1674.1, 1132.1, 655.2, 400.7, 199.3, 57.7, 52.2, 50.0
CHO	0.06	CO	0.56	-0.15	1.08	2792.1, 1674.1, 1132.1, 655.2, 400.7, 199.3, 57.7, 52.2, 50.0
HCOO	0.06	None	0.00	-0.08	-1.34	2952.0, 1519.0, 1308.4, 1301.4, 981.1, 745.5, 289.1, 280.1, 269.3, 94.9, 84.2, 50.7

Adsorbate	Coverage	Coadsorbate	Coadsorbate coverage	$E_{int}(\theta_i)[eV]$	Formation energy [eV]	Frequencies [cm^{-1}]
HCOO	0.06	CO	0.50	-0.24	-0.47	2952.0, 1519.0, 1308.4, 1301.4, 981.1, 745.5, 289.1, 280.1, 269.3, 94.9, 84.2, 50.7
HCOO	0.06	CO	0.56	-0.17	0.79	2952.0, 1519.0, 1308.4, 1301.4, 981.1, 745.5, 289.1, 280.1, 269.3, 94.9, 84.2, 50.7
CO2	0.06	None	0.00	-0.07	-1.06	2373.3, 1315.1, 619.1, 607.5, 77.1, 50.0, 50.0, 50.0, 50.0
CO2	0.06	CO	0.06	-0.10	-1.09	2373.3, 1315.1, 619.1, 607.5, 77.1, 50.0, 50.0, 50.0, 50.0
CO2	0.06	CO	0.12	-0.13	-1.09	2373.3, 1315.1, 619.1, 607.5, 77.1, 50.0, 50.0, 50.0, 50.0
CO2	0.06	CO	0.25	-0.19	-1.10	2373.3, 1315.1, 619.1, 607.5, 77.1, 50.0, 50.0, 50.0, 50.0
CO2	0.06	CO	0.56	-0.15	1.12	2373.3, 1315.1, 619.1, 607.5, 77.1, 50.0, 50.0, 50.0, 50.0
CO2	0.06	CO	0.62	-0.15	0.19	2373.3, 1315.1, 619.1, 607.5, 77.1, 50.0, 50.0, 50.0, 50.0
H	0.06	None	0.00	-0.01	-0.14	1067.4, 799.3, 777.7

Adsorbate	Coverage	Coadsorbate	Coadsorbate coverage	$E_{int}(\theta_i)[eV]$	Formation energy [eV]	Frequencies [cm^{-1}]
H	0.06	CO	0.44	-0.19	0.04	1067.4, 799.3, 777.7
H	0.06	CO	0.50	-0.21	0.05	1067.4, 799.3, 777.7
H	0.06	CO	0.62	-0.14	0.33	1067.4, 799.3, 777.7
OH-H	0.06	None	0.00	0.06	1.02	3750.6, 845.0, 748.3, 656.6, 417.0, 373.2, 113.1, 76.6
OH-H	0.06	CO	0.56	-0.15	1.14	3750.6, 845.0, 748.3, 656.6, 417.0, 373.2, 113.1, 76.6
OH-H	0.06	CO	0.62	-0.07	1.36	3750.6, 845.0, 748.3, 656.6, 417.0, 373.2, 113.1, 76.6
O-H	0.06	None	0.00	0.12	1.85	967.5, 504.2, 398.1, 238.5, 209.4
O-H	0.06	CO	0.56	-0.07	2.38	967.5, 504.2, 398.1, 238.5, 209.4
O-H	0.06	CO	0.62	0.02	2.91	967.5, 504.2, 398.1, 238.5, 209.4
O-OHH	0.06	None	0.00	0.04	0.63	3835.7, 1410.5, 1290.7, 760.9, 692.7, 483.9, 423.0, 357.3, 254.7, 158.6, 99.2
O-OHH	0.06	CO	0.38	-0.12	0.82	3835.7, 1410.5, 1290.7, 760.9, 692.7, 483.9, 423.0, 357.3, 254.7, 158.6, 99.2

Adsorbate	Coverage	Coadsorbate	Coadsorbate coverage	$E_{int}(\theta_i)[eV]$	Formation energy [eV]	Frequencies [cm^{-1}]
O-OHH	0.06	CO	0.56	-0.14	1.31	3835.7, 1410.5, 1290.7, 760.9, 692.7, 483.9, 423.0, 357.3, 254.7, 158.6, 99.2
CO-O	0.06	None	0.00	0.06	1.04	1991.3, 537.2, 342.8, 341.2, 303.6, 235.1, 79.2, 53.3
CO-O	0.06	CO	0.50	-0.12	1.49	1991.3, 537.2, 342.8, 341.2, 303.6, 235.1, 79.2, 53.3
CO-O	0.06	CO	0.56	-0.10	1.95	1991.3, 537.2, 342.8, 341.2, 303.6, 235.1, 79.2, 53.3
CO-OH	0.06	None	0.00	0.01	0.13	3662.1, 1897.9, 865.3, 609.3, 405.4, 323.5, 289.2, 241.9, 106.9, 59.4, 50.0
CO-OH	0.06	CO	0.50	-0.17	0.61	3662.1, 1897.9, 865.3, 609.3, 405.4, 323.5, 289.2, 241.9, 106.9, 59.4, 50.0
CO-OH	0.06	CO	0.56	-0.19	0.59	3662.1, 1897.9, 865.3, 609.3, 405.4, 323.5, 289.2, 241.9, 106.9, 59.4, 50.0
CO-HO	0.06	None	0.00	0.02	0.28	3654.4, 1680.7, 1119.8, 780.2, 631.6, 370.8, 245.2, 179.1, 54.3, 50.0, 50.0

Adsorbate	Coverage	Coadsorbate	Coadsorbate coverage	$E_{int}(\theta_i)[eV]$	Formation energy [eV]	Frequencies [cm^{-1}]
CO-HO	0.06	CO	0.25	-0.11	0.28	3654.4, 1680.7, 1119.8, 780.2, 631.6, 370.8, 245.2, 179.1, 54.3, 50.0, 50.0
CO-HO	0.06	CO	0.50	-0.18	0.51	3654.4, 1680.7, 1119.8, 780.2, 631.6, 370.8, 245.2, 179.1, 54.3, 50.0, 50.0
CO-HO	0.06	CO	0.62	-0.11	0.81	3654.4, 1680.7, 1119.8, 780.2, 631.6, 370.8, 245.2, 179.1, 54.3, 50.0, 50.0
COO-H	0.06	None	0.00	0.05	0.79	1777.8, 1110.9, 807.5, 652.7, 611.2, 467.7, 286.0, 164.6, 97.1, 74.6, 50.0
COO-H	0.06	CO	0.06	0.02	0.76	1777.8, 1110.9, 807.5, 652.7, 611.2, 467.7, 286.0, 164.6, 97.1, 74.6, 50.0
COO-H	0.06	CO	0.12	-0.01	0.78	1777.8, 1110.9, 807.5, 652.7, 611.2, 467.7, 286.0, 164.6, 97.1, 74.6, 50.0
COO-H	0.06	CO	0.19	-0.05	0.68	1777.8, 1110.9, 807.5, 652.7, 611.2, 467.7, 286.0, 164.6, 97.1, 74.6, 50.0
COO-H	0.06	CO	0.25	-0.07	0.76	1777.8, 1110.9, 807.5, 652.7, 611.2, 467.7, 286.0, 164.6, 97.1, 74.6, 50.0

Adsorbate	Coverage	Coadsorbate	Coadsorbate coverage	$E_{int}(\theta_i)[eV]$	Formation energy [eV]	Frequencies [cm^{-1}]
COO-H	0.06	CO	0.31	-0.09	0.76	1777.8, 1110.9, 807.5, 652.7, 611.2, 467.7, 286.0, 164.6, 97.1, 74.6, 50.0
COO-H	0.06	CO	0.50	-0.08	2.19	1777.8, 1110.9, 807.5, 652.7, 611.2, 467.7, 286.0, 164.6, 97.1, 74.6, 50.0
COO-OHH	0.06	None	0.00	-0.02	-0.30	3831.7, 1685.8, 1619.4, 1251.0, 1128.5, 832.7, 745.9, 611.2, 431.3, 400.6, 354.3, 260.6, 245.9, 120.2, 113.2, 85.9, 55.6
COO-OHH	0.06	CO	0.31	-0.16	-0.32	3831.7, 1685.8, 1619.4, 1251.0, 1128.5, 832.7, 745.9, 611.2, 431.3, 400.6, 354.3, 260.6, 245.9, 120.2, 113.2, 85.9, 55.6
COO-OHH	0.06	CO	0.38	-0.14	0.52	3831.7, 1685.8, 1619.4, 1251.0, 1128.5, 832.7, 745.9, 611.2, 431.3, 400.6, 354.3, 260.6, 245.9, 120.2, 113.2, 85.9, 55.6
CO-H	0.06	None	0.00	0.03	0.45	1908.8, 1206.5, 656.5, 323.1, 301.9, 50.0, 50.0, 50.0
CO-H	0.06	CO	0.56	-0.18	0.73	1908.8, 1206.5, 656.5, 323.1, 301.9, 50.0, 50.0, 50.0

Adsorbate	Coverage	Coadsorbate	Coadsorbate coverage	$E_{int}(\theta_i)[eV]$	Formation energy [eV]	Frequencies [cm^{-1}]
CO-H	0.06	CO	0.62	-0.11	0.86	1908.8, 1206.5, 656.5, 323.1, 301.9, 50.0, 50.0, 50.0
HCO-O	0.06	None	0.00	0.08	1.26	3187.5, 1654.5, 1250.0, 946.1, 624.9, 440.4, 385.9, 207.8, 176.1, 89.2, 66.4
HCO-O	0.06	CO	0.31	-0.07	1.21	3187.5, 1654.5, 1250.0, 946.1, 624.9, 440.4, 385.9, 207.8, 176.1, 89.2, 66.4
HCO-O	0.06	CO	0.38	-0.09	1.41	3187.5, 1654.5, 1250.0, 946.1, 624.9, 440.4, 385.9, 207.8, 176.1, 89.2, 66.4
H-COO	0.06	None	0.00	-0.01	-0.22	2069.2, 1473.0, 1180.3, 956.4, 672.8, 407.7, 188.4, 114.7, 58.7, 50.0, 50.0
H-COO	0.06	CO	0.38	-0.18	-0.14	2069.2, 1473.0, 1180.3, 956.4, 672.8, 407.7, 188.4, 114.7, 58.7, 50.0, 50.0
H-COO	0.06	CO	0.44	-0.21	-0.36	2069.2, 1473.0, 1180.3, 956.4, 672.8, 407.7, 188.4, 114.7, 58.7, 50.0, 50.0
H-H	0.06	None	0.00	0.04	0.66	1361.2, 1353.3, 588.5, 478.0, 234.1
H-H	0.06	CO	0.06	0.01	0.60	1361.2, 1353.3, 588.5, 478.0, 234.1

H-H	0.06	CO	0.44	-0.15	0.71	1361.2, 1353.3, 588.5, 478.0, 234.1

S6.8 Cu_7 Elementary Steps

These are the elementary steps used in the microkinetic modeling for Cu_7 cluster.

$$*_s + CO_{(g)} \leftrightarrow CO^{*_s} \tag{14}$$

$$*_s + H_2O_{(g)} \leftrightarrow H_2O^{*_s} \tag{15}$$

$$CO_{2(g)} + *_s \leftrightarrow CO_2^{*_s} \tag{16}$$

$$H_2O^{*_s} + *_s \leftrightarrow OH{-}H^{*_s} + *_s \rightarrow H^{*_s} + OH^{*_s} \tag{17}$$

$$OH^{*_s} + *_s \leftrightarrow O{-}H^{*_s} + *_s \rightarrow O^{*_s} + H^{*_s} \tag{18}$$

$$OH^{*_s} + OH^{*_s} \leftrightarrow O{-}OHH^{*_s} + *_s \rightarrow H_2O^{*_s} + O^{*_s} \tag{19}$$

$$CO^{*_s} + O^{*_s} \leftrightarrow CO{-}O^{*_s} + *_s \rightarrow CO_2^{*_s} + *_s \tag{20}$$

$$CO^{*_s} + OH^{*_s} \leftrightarrow CO{-}OH^{*_s} + *_s \rightarrow COOH^{*_s} + *_s \tag{21}$$

$$COOH^{*_s} \leftrightarrow CO{-}HO^{*_s} \rightarrow COHO^{*_s} \tag{22}$$

$$COHO^{*_s} + *_s \leftrightarrow COO{-}H^{*_s} + *_s \rightarrow CO_2^{*_s} + H^{*_s} \tag{23}$$

$$COHO^{*_s} + OH^{*_s} \leftrightarrow COO{-}OHH^{*_s} + *_s \rightarrow CO_2^{*_s} + H_2O^{*_s} \tag{24}$$

$$H^{*_s} + H^{*_s} \leftrightarrow H{-}H^{*_s} + *_s \rightarrow H_{2(g)} + *_s + *_s \tag{25}$$

S6.9 Cu_7 Interaction Parameters

All unlisted $\epsilon_{i,j}$ in Table S8 are assumed to be zero.

Table S8: Lateral interaction parameters $\epsilon_{i,j}$ on Cu_7.

i	j	$\epsilon_{i,j}$
CO	CO	0.20
CO	CO_2	0.81
CO	COHO	0.94
CO	COOH	0.45
CO	H_2O	-0.16
CO	H	0.15
CO	OH	0.81
CO	O	-0.29
CO	CO-HO	1.95
CO	CO-OH	0.32
CO	CO-O	0.58
CO	COO-H	-0.29
CO	COO-OHH	1.17
CO	H-H	-0.33
CO	O-H	0.97
CO	O-OHH	0.32
CO	OH-H	0.78

S6.10 Cu_7 Energies and Frequencies

Table S9 summarizes the adsorbates, coadsorbates, their coverages, integral formation energies (E_{int}), formation energies, and vibrational frequencies on Cu_7.

Table S9: Adsorbates, coadsorbates, formation energies, and frequencies for Cu_7.

Adsorbate	Coverage	Coadsorbate	Coadsorbate coverage	$E_{int}(\theta_i)[eV]$	Formation energy [eV]	Frequencies [cm^{-1}]
CO(g)	0.00	None	0.00	0.00	0.00	2165.5
CO2(g)	0.00	None	0.00	-0.84	-0.84	2401.6, 1328.9, 642.0, 642.0
H2(g)	0.00	None	0.00	0.00	0.00	4403.9
H2O(g)	0.00	None	0.00	0.00	0.00	3898.9, 3794.3, 1580.8
CO	0.14	None	0.00	-0.12	-0.83	2075.3, 328.9, 261.8, 255.1, 50.0, 50.0
CO	0.29	None	0.00	-0.24	-0.82	2075.3, 328.9, 261.8, 255.1, 50.0, 50.0
CO	0.43	None	0.00	-0.35	-0.81	2075.3, 328.9, 261.8, 255.1, 50.0, 50.0
CO	0.57	None	0.00	-0.46	-0.79	2075.3, 328.9, 261.8, 255.1, 50.0, 50.0
CO	0.71	None	0.00	-0.57	-0.76	2075.3, 328.9, 261.8, 255.1, 50.0, 50.0
CO	0.86	None	0.00	-0.68	-0.74	2075.3, 328.9, 261.8, 255.1, 50.0, 50.0
H2O	0.14	None	0.00	-0.06	-0.42	3732.5, 3639.3, 1565.2, 513.5, 444.7, 177.9, 124.9, 50.0, 50.0
H2O	0.14	CO	0.14	-0.18	-0.42	3732.5, 3639.3, 1565.2, 513.5, 444.7, 177.9, 124.9, 50.0, 50.0

Adsorbate	Coverage	Coadsorbate	Coadsorbate coverage	$E_{int}(\theta_i)[eV]$	Formation energy [eV]	Frequencies [cm^{-1}]
H2O	0.14	CO	0.29	-0.30	-0.42	3732.5, 3639.3, 1565.2, 513.5, 444.7, 177.9, 124.9, 50.0, 50.0
H2O	0.14	CO	0.57	-0.52	-0.45	3732.5, 3639.3, 1565.2, 513.5, 444.7, 177.9, 124.9, 50.0, 50.0
H2O	0.14	CO	0.71	-0.63	-0.44	3732.5, 3639.3, 1565.2, 513.5, 444.7, 177.9, 124.9, 50.0, 50.0
OH	0.14	None	0.00	-0.06	-0.41	3690.4, 698.7, 628.1, 380.9, 275.3, 118.4
OH	0.14	CO	0.29	-0.28	-0.31	3690.4, 698.7, 628.1, 380.9, 275.3, 118.4
OH	0.14	CO	0.71	-0.59	-0.13	3690.4, 698.7, 628.1, 380.9, 275.3, 118.4
O	0.14	None	0.00	0.08	0.56	442.7, 360.3, 349.4
O	0.14	CO	0.29	-0.17	0.51	442.7, 360.3, 349.4
O	0.14	CO	0.86	-0.61	0.47	442.7, 360.3, 349.4
COOH	0.14	None	0.00	-0.11	-0.80	3590.7, 1780.8, 1151.1, 745.5, 493.1, 434.8, 311.6, 283.1, 232.6, 130.9, 71.5, 50.0

Adsorbate	Coverage	Coadsorbate	Coadsorbate coverage	$E_{int}(\theta_i)[eV]$	Formation energy [eV]	Frequencies [cm^{-1}]
COOH	0.14	CO	0.14	-0.23	-0.79	3590.7, 1780.8, 1151.1, 745.5, 493.1, 434.8, 311.6, 283.1, 232.6, 130.9, 71.5, 50.0
COOH	0.14	CO	0.29	-0.35	-0.74	3590.7, 1780.8, 1151.1, 745.5, 493.1, 434.8, 311.6, 283.1, 232.6, 130.9, 71.5, 50.0
COOH	0.14	CO	0.71	-0.66	-0.63	3590.7, 1780.8, 1151.1, 745.5, 493.1, 434.8, 311.6, 283.1, 232.6, 130.9, 71.5, 50.0
COHO	0.14	None	0.00	-0.09	-0.65	3625.7, 1747.5, 1295.8, 993.5, 634.6, 594.3, 394.9, 246.4, 208.0, 52.3, 50.0, 50.0
COHO	0.14	CO	0.14	-0.21	-0.63	3625.7, 1747.5, 1295.8, 993.5, 634.6, 594.3, 394.9, 246.4, 208.0, 52.3, 50.0, 50.0
COHO	0.14	CO	0.29	-0.33	-0.66	3625.7, 1747.5, 1295.8, 993.5, 634.6, 594.3, 394.9, 246.4, 208.0, 52.3, 50.0, 50.0
COHO	0.14	CO	0.71	-0.62	-0.33	3625.7, 1747.5, 1295.8, 993.5, 634.6, 594.3, 394.9, 246.4, 208.0, 52.3, 50.0, 50.0

Adsorbate	Coverage	Coadsorbate	Coadsorbate coverage	$E_{int}(\theta_i)[eV]$	Formation energy [eV]	Frequencies [cm^{-1}]
CHO	0.14	None	0.00	-0.07	-0.51	2647.3, 1654.5, 1121.5, 680.7, 459.9, 243.5, 101.7, 52.5, 50.0
CHO	0.14	CO	0.14	-0.19	-0.48	2647.3, 1654.5, 1121.5, 680.7, 459.9, 243.5, 101.7, 52.5, 50.0
CHO	0.14	CO	0.57	-0.53	-0.46	2647.3, 1654.5, 1121.5, 680.7, 459.9, 243.5, 101.7, 52.5, 50.0
CHO	0.14	CO	0.71	-0.63	-0.40	2647.3, 1654.5, 1121.5, 680.7, 459.9, 243.5, 101.7, 52.5, 50.0
HCOO	0.14	None	0.00	-0.28	-1.97	2923.3, 1534.7, 1331.0, 1327.1, 1002.5, 754.2, 328.7, 301.6, 283.6, 102.8, 94.8, 50.0
HCOO	0.14	CO	0.14	-0.40	-1.95	2923.3, 1534.7, 1331.0, 1327.1, 1002.5, 754.2, 328.7, 301.6, 283.6, 102.8, 94.8, 50.0
HCOO	0.14	CO	0.71	-0.83	-1.84	2923.3, 1534.7, 1331.0, 1327.1, 1002.5, 754.2, 328.7, 301.6, 283.6, 102.8, 94.8, 50.0

Adsorbate	Coverage	Coadsorbate	Coadsorbate coverage	$E_{int}(\theta_i)[eV]$	Formation energy [eV]	Frequencies [cm^{-1}]
CO2	0.14	None	0.00	-0.15	-1.05	2369.8, 1317.1, 599.0, 579.7, 78.6, 74.6, 50.0, 50.0, 50.0
CO2	0.14	CO	0.14	-0.27	-1.05	2369.8, 1317.1, 599.0, 579.7, 78.6, 74.6, 50.0, 50.0, 50.0
CO2	0.14	CO	0.71	-0.68	-0.77	2369.8, 1317.1, 599.0, 579.7, 78.6, 74.6, 50.0, 50.0, 50.0
H	0.14	None	0.00	-0.03	-0.24	1084.4, 770.2, 753.5
H	0.14	CO	0.43	-0.38	-0.23	1084.4, 770.2, 753.5
H	0.14	CO	0.86	-0.70	-0.14	1084.4, 770.2, 753.5
OH-H	0.14	None	0.00	0.04	0.27	3703.4, 915.3, 565.5, 531.0, 484.4, 341.4, 259.4, 186.8
OH-H	0.14	CO	0.29	-0.19	0.35	3703.4, 915.3, 565.5, 531.0, 484.4, 341.4, 259.4, 186.8
OH-H	0.14	CO	0.43	-0.30	0.32	3703.4, 915.3, 565.5, 531.0, 484.4, 341.4, 259.4, 186.8
OH-H	0.14	CO	0.71	-0.49	0.54	3703.4, 915.3, 565.5, 531.0, 484.4, 341.4, 259.4, 186.8

Adsorbate	Coverage	Coadsorbate	Coadsorbate coverage	$E_{int}(\theta_i)[eV]$	Formation energy [eV]	Frequencies [cm^{-1}]
O-OHH	0.14	None	0.00	-0.01	-0.05	3837.5, 1467.9, 1297.0, 884.8, 707.2, 467.9, 396.0, 355.6, 263.8, 156.5, 77.0
O-OHH	0.14	CO	0.14	-0.13	-0.06	3837.5, 1467.9, 1297.0, 884.8, 707.2, 467.9, 396.0, 355.6, 263.8, 156.5, 77.0
O-OHH	0.14	CO	0.43	-0.35	-0.01	3837.5, 1467.9, 1297.0, 884.8, 707.2, 467.9, 396.0, 355.6, 263.8, 156.5, 77.0
O-OHH	0.14	CO	0.71	-0.56	0.08	3837.5, 1467.9, 1297.0, 884.8, 707.2, 467.9, 396.0, 355.6, 263.8, 156.5, 77.0
CO-OH	0.14	None	0.00	-0.07	-0.48	3718.7, 1911.9, 905.7, 624.3, 384.6, 333.8, 287.5, 230.7, 143.2, 60.4, 50.0
CO-OH	0.14	CO	0.14	-0.19	-0.47	3718.7, 1911.9, 905.7, 624.3, 384.6, 333.8, 287.5, 230.7, 143.2, 60.4, 50.0
CO-OH	0.14	CO	0.29	-0.30	-0.43	3718.7, 1911.9, 905.7, 624.3, 384.6, 333.8, 287.5, 230.7, 143.2, 60.4, 50.0
CO-OH	0.14	CO	0.43	-0.41	-0.44	3718.7, 1911.9, 905.7, 624.3, 384.6, 333.8, 287.5, 230.7, 143.2, 60.4, 50.0

Adsorbate	Coverage	Coadsorbate	Coadsorbate coverage	$E_{int}(\theta_i)[eV]$	Formation energy [eV]	Frequencies [cm^{-1}]
CO-OH	0.14	CO	0.57	-0.52	-0.42	3718.7, 1911.9, 905.7, 624.3, 384.6, 333.8, 287.5, 230.7, 143.2, 60.4, 50.0
CO-OH	0.14	CO	0.71	-0.62	-0.35	3718.7, 1911.9, 905.7, 624.3, 384.6, 333.8, 287.5, 230.7, 143.2, 60.4, 50.0
CO-HO	0.14	None	0.00	-0.06	-0.45	3615.7, 1796.0, 1143.2, 709.7, 538.2, 425.1, 374.6, 246.1, 177.0, 71.8, 50.0
CO-HO	0.14	CO	0.29	-0.30	-0.43	3615.7, 1796.0, 1143.2, 709.7, 538.2, 425.1, 374.6, 246.1, 177.0, 71.8, 50.0
CO-HO	0.14	CO	0.71	-0.54	0.18	3615.7, 1796.0, 1143.2, 709.7, 538.2, 425.1, 374.6, 246.1, 177.0, 71.8, 50.0
COO-OHH	0.14	None	0.00	-0.15	-1.03	3822.2, 1732.3, 1660.8, 1328.4, 1257.0, 821.1, 717.7, 555.2, 509.2, 480.0, 361.8, 261.6, 171.6, 146.2, 82.3, 62.9, 50.0
COO-OHH	0.14	CO	0.14	-0.26	-0.98	3822.2, 1732.3, 1660.8, 1328.4, 1257.0, 821.1, 717.7, 555.2, 509.2, 480.0, 361.8, 261.6, 171.6, 146.2, 82.3, 62.9, 50.0

Adsorbate	Coverage	Coadsorbate	Coadsorbate coverage	$E_{int}(\theta_i)[eV]$	Formation energy [eV]	Frequencies [cm^{-1}]
COO-OHH	0.14	CO	0.71	-0.66	-0.64	3822.2, 1732.3, 1660.8, 1328.4, 1257.0, 821.1, 717.7, 555.2, 509.2, 480.0, 361.8, 261.6, 171.6, 146.2, 82.3, 62.9, 50.0
HCO-O	0.14	None	0.00	0.08	0.59	2971.8, 1773.6, 1211.6, 734.8, 496.3, 401.2, 334.9, 254.2, 222.5, 138.5, 50.0
HCO-O	0.14	CO	0.29	-0.16	0.59	2971.8, 1773.6, 1211.6, 734.8, 496.3, 401.2, 334.9, 254.2, 222.5, 138.5, 50.0
HCO-O	0.14	CO	0.71	-0.48	0.66	2971.8, 1773.6, 1211.6, 734.8, 496.3, 401.2, 334.9, 254.2, 222.5, 138.5, 50.0
H-H	0.14	None	0.00	0.08	0.54	1133.7, 1131.1, 903.3, 857.6, 376.6
H-H	0.14	CO	0.14	-0.04	0.54	1133.7, 1131.1, 903.3, 857.6, 376.6
H-H	0.14	CO	0.57	-0.40	0.43	1133.7, 1131.1, 903.3, 857.6, 376.6
H-H	0.14	CO	0.71	-0.50	0.47	1133.7, 1131.1, 903.3, 857.6, 376.6
O-H	0.14	None	0.00	0.17	1.16	832.6, 576.0, 559.3, 407.6, 343.5
O-H	0.14	CO	0.43	-0.17	1.29	832.6, 576.0, 559.3, 407.6, 343.5
O-H	0.14	CO	0.57	-0.27	1.31	832.6, 576.0, 559.3, 407.6, 343.5
O-H	0.14	CO	0.71	-0.36	1.49	832.6, 576.0, 559.3, 407.6, 343.5

Adsorbate	Coverage	Coadsorbate	Coadsorbate coverage	$E_{int}(\theta_i)[eV]$	Formation energy [eV]	Frequencies [cm^{-1}]
CO-O	0.14	None	0.00	0.07	0.45	1980.8, 526.4, 377.0, 344.9, 316.5, 226.5, 112.7, 50.0
CO-O	0.14	CO	0.14	-0.05	0.45	1980.8, 526.4, 377.0, 344.9, 316.5, 226.5, 112.7, 50.0
CO-O	0.14	CO	0.71	-0.47	0.66	1980.8, 526.4, 377.0, 344.9, 316.5, 226.5, 112.7, 50.0
COO-H	0.14	None	0.00	0.05	0.36	1770.9, 1111.5, 855.3, 593.0, 542.5, 473.2, 286.0, 147.2, 84.8, 79.0, 50.0
COO-H	0.14	CO	0.29	-0.19	0.36	1770.9, 1111.5, 855.3, 593.0, 542.5, 473.2, 286.0, 147.2, 84.8, 79.0, 50.0
COO-H	0.14	CO	0.71	-0.53	0.30	1770.9, 1111.5, 855.3, 593.0, 542.5, 473.2, 286.0, 147.2, 84.8, 79.0, 50.0
CO-H	0.14	None	0.00	0.03	0.19	1903.8, 1655.3, 917.9, 342.9, 314.9, 263.3, 50.0, 50.0
CO-H	0.14	CO	0.43	-0.32	0.22	1903.8, 1655.3, 917.9, 342.9, 314.9, 263.3, 50.0, 50.0

Adsorbate	Coverage	Coadsorbate	Coadsorbate coverage	$E_{int}(\theta_i)[eV]$	Formation energy [eV]	Frequencies [cm^{-1}]
CO-H	0.14	CO	0.71	-0.51	0.39	1903.8, 1655.3, 917.9, 342.9, 314.9, 263.3, 50.0, 50.0
H-COO	0.14	None	0.00	-0.08	-0.55	2184.7, 1568.0, 1194.6, 943.4, 634.9, 443.3, 259.6, 154.4, 63.8, 55.5, 50.0
H-COO	0.14	CO	0.14	-0.17	-0.33	2184.7, 1568.0, 1194.6, 943.4, 634.9, 443.3, 259.6, 154.4, 63.8, 55.5, 50.0
H-COO	0.14	CO	0.29	-0.28	-0.30	2184.7, 1568.0, 1194.6, 943.4, 634.9, 443.3, 259.6, 154.4, 63.8, 55.5, 50.0
H-COO	0.14	CO	0.57	-0.51	-0.36	2184.7, 1568.0, 1194.6, 943.4, 634.9, 443.3, 259.6, 154.4, 63.8, 55.5, 50.0

S6.11 Cu_4 Elementary Steps

These are the elementary steps used in the microkinetic modeling for Cu_4 cluster.

$$*_s + CO_{(g)} \leftrightarrow CO^{*s} \tag{26}$$

$$*_s + H_2O_{(g)} \leftrightarrow H_2O^{*s} \tag{27}$$

$$*_s + CO_{2(g)} \leftrightarrow CO_2^{*s} \tag{28}$$

$$H_2O^{*s} + *_t \leftrightarrow OH{-}H^{*s} + *_t \rightarrow H^{*t} + OH^{*s} \tag{29}$$

$$OH^{*s} + *_t \leftrightarrow O{-}H^{*s} + *_t \rightarrow O^{*s} + H^{*t} \tag{30}$$

$$OH^{*s} + OH^{*s} \leftrightarrow O{-}OHH^{*s} + *_s \rightarrow H_2O^{*s} + O^{*s} \tag{31}$$

$$CO^{*s} + O^{*s} \leftrightarrow CO{-}O^{*s} + *_s \rightarrow CO_2^{*s} + *_s \tag{32}$$

$$CO^{*s} + OH^{*s} \leftrightarrow CO{-}OH^{*s} + *_s \rightarrow COOH^{*s} + *_s \tag{33}$$

$$COOH^{*s} \leftrightarrow CO{-}HO^{*s} \rightarrow COHO^{*s} \tag{34}$$

$$COHO^{*s} + *_s \leftrightarrow COO{-}H^{*s} + *_s \rightarrow CO_2^{*s} + H^{*s} \tag{35}$$

$$COHO^{*s} + OH^{*s} \leftrightarrow COO{-}OHH^{*s} + *_s \rightarrow CO_2^{*s} + H_2O^{*s} \tag{36}$$

$$H^{*s} + H^{*t} \leftrightarrow H{-}H^{*s} + *_t \rightarrow H_{2(g)} + *_s + *_t \tag{37}$$

$$H^{*t} + *_s \leftrightarrow H{-}^{*t} + *_s \rightarrow H^{*s} + *_t \tag{38}$$

S6.12 Cu_4 Interaction Parameters

All unlisted $\epsilon_{i,j}$ in Table S10 are assumed to be zero.

Table S10: Lateral interaction parameters $\epsilon_{i,j}$ on Cu_4.

i	j	$\epsilon_{i,j}$
CO	CO	0.18
CO	CO_2	-0.21
CO	COHO	-0.15
CO	COOH	0.35
CO	H_2O	-0.22
CO	H	-0.09
CO	OH	0.25
CO	O	0.21
CO	CO-HO	0.89
CO	CO-OH	0.39
CO	CO-O	0.68
CO	COO-H	0.25
CO	COO-OHH	1.27
CO	H-H	0.33
CO	O-H	0.64
CO	O-OHH	0.68
CO	OH-H	0.58

S6.13 Cu_4 Energies and Frequencies

Table S11 summarizes the adsorbates, coadsorbates, their coverages, integral formation energies (E_{int}), formation energies, and vibrational frequencies on Cu_4.

Table S11: Adsorbates, coadsorbates, formation energies, and frequencies for Cu_4.

Adsorbate	Coverage	Coadsorbate	Coadsorbate coverage	$E_{int}(\theta_i)[eV]$	Formation energy [eV]	Frequencies [cm^{-1}]
CO(g)	0.00	None	0.00	0.00	0.00	2165.5
CO2(g)	0.00	None	0.00	-0.84	-0.84	2401.6, 1328.9, 642.0, 642.0
H2(g)	0.00	None	0.00	0.00	0.00	4403.9
H2O(g)	0.00	None	0.00	0.00	0.00	3898.9, 3794.3, 1580.8
CO	0.25	None	0.00	-0.23	-0.91	2078.3, 333.0, 277.4, 239.9, 50.0, 50.0
CO	0.50	None	0.00	-0.44	-0.86	2078.3, 333.0, 277.4, 239.9, 50.0, 50.0
CO	0.75	None	0.00	-0.65	-0.82	2078.3, 333.0, 277.4, 239.9, 50.0, 50.0
CO	1.00	None	0.00	-0.86	-0.83	2078.3, 333.0, 277.4, 239.9, 50.0, 50.0
H2O	0.25	None	0.00	-0.11	-0.42	3799.9, 3696.8, 1578.3, 480.1, 455.2, 169.0, 54.9, 50.0
H2O	0.25	CO	0.50	-0.56	-0.46	3799.9, 3696.8, 1578.3, 480.1, 455.2, 169.0, 54.9, 50.0
H2O	0.25	CO	0.75	-0.77	-0.49	3799.9, 3696.8, 1578.3, 480.1, 455.2, 169.0, 54.9, 50.0
OH	0.25	None	0.00	-0.09	-0.36	3778.7, 553.8, 477.9, 370.1, 233.8, 171.8

Adsorbate	Coverage	Coadsorbate	Coadsorbate coverage	$E_{int}(\theta_i)[eV]$	Formation energy [eV]	Frequencies [cm^{-1}]
OH	0.25	CO	0.25	-0.31	-0.31	3778.7, 553.8, 477.9, 370.1, 233.8, 171.8
OH	0.25	CO	1.00	-0.90	-0.17	3778.7, 553.8, 477.9, 370.1, 233.8, 171.8
O	0.25	None	0.00	0.11	0.46	449.6, 352.3, 324.7
O	0.25	CO	0.50	-0.32	0.47	449.6, 352.3, 324.7
O	0.25	CO	1.00	-0.71	0.62	449.6, 352.3, 324.7
COOH	0.25	None	0.00	-0.21	-0.86	3588.1, 1786.9, 1142.6, 751.4, 503.8, 446.2, 320.8, 284.9, 230.6, 129.5, 66.1, 50.0
COOH	0.25	CO	0.25	-0.45	-0.86	3588.1, 1786.9, 1142.6, 751.4, 503.8, 446.2, 320.8, 284.9, 230.6, 129.5, 66.1, 50.0
COOH	0.25	CO	0.50	-0.65	-0.86	3588.1, 1786.9, 1142.6, 751.4, 503.8, 446.2, 320.8, 284.9, 230.6, 129.5, 66.1, 50.0
COOH	0.25	CO	0.75	-0.82	-0.69	3588.1, 1786.9, 1142.6, 751.4, 503.8, 446.2, 320.8, 284.9, 230.6, 129.5, 66.1, 50.0

Adsorbate	Coverage	Coadsorbate	Coadsorbate coverage	$E_{int}(\theta_i)[eV]$	Formation energy [eV]	Frequencies [cm^{-1}]
COHO	0.25	None	0.00	-0.16	-0.64	3623.0, 1739.6, 1280.1, 1000.4, 633.9, 617.3, 403.1, 247.1, 202.3, 56.5, 50.0, 50.0
COHO	0.25	CO	0.50	-0.60	-0.66	3623.0, 1739.6, 1280.1, 1000.4, 633.9, 617.3, 403.1, 247.1, 202.3, 56.5, 50.0, 50.0
COHO	0.25	CO	0.75	-0.82	-0.68	3623.0, 1739.6, 1280.1, 1000.4, 633.9, 617.3, 403.1, 247.1, 202.3, 56.5, 50.0, 50.0
CHO	0.25	None	0.00	-0.14	-0.58	2708.9, 1693.8, 1220.3, 691.8, 444.4, 220.8, 89.2, 50.0, 50.0
CHO	0.25	CO	0.25	-0.37	-0.54	2708.9, 1693.8, 1220.3, 691.8, 444.4, 220.8, 89.2, 50.0, 50.0
CHO	0.25	CO	0.50	-0.58	-0.56	2708.9, 1693.8, 1220.3, 691.8, 444.4, 220.8, 89.2, 50.0, 50.0
CHO	0.25	CO	0.75	-0.77	-0.49	2708.9, 1693.8, 1220.3, 691.8, 444.4, 220.8, 89.2, 50.0, 50.0
HCOO	0.25	None	0.00	-0.51	-2.04	2954.0, 1541.5, 1334.5, 1332.5, 1015.1, 756.4, 330.0, 303.8, 286.9, 103.4, 93.2, 50.0

Adsorbate	Coverage	Coadsorbate	Coadsorbate coverage	$E_{int}(\theta_i)[eV]$	Formation energy [eV]	Frequencies [cm^{-1}]
HCOO	0.25	CO	0.25	-0.74	-2.05	2954.0, 1541.5, 1334.5, 1332.5, 1015.1, 756.4, 330.0, 303.8, 286.9, 103.4, 93.2, 50.0
HCOO	0.25	CO	0.50	-0.96	-2.10	2954.0, 1541.5, 1334.5, 1332.5, 1015.1, 756.4, 330.0, 303.8, 286.9, 103.4, 93.2, 50.0
CO2	0.25	None	0.00	-0.26	-1.04	2371.7, 1318.2, 596.3, 575.1, 82.4, 69.4, 50.0, 50.0, 50.0
CO2	0.25	CO	0.25	-0.49	-1.05	2371.7, 1318.2, 596.3, 575.1, 82.4, 69.4, 50.0, 50.0, 50.0
CO2	0.25	CO	0.50	-0.71	-1.07	2371.7, 1318.2, 596.3, 575.1, 82.4, 69.4, 50.0, 50.0, 50.0
H	0.25	None	0.00	-0.05	-0.22	1064.8, 742.1, 630.6
H	0.25	CO	0.25	-0.28	-0.22	1064.8, 742.1, 630.6
H	0.25	CO	0.75	-0.71	-0.24	1064.8, 742.1, 630.6
H	0.25	CO	1.00	-0.92	-0.25	1064.8, 742.1, 630.6

Adsorbate	Coverage	Coadsorbate	Coadsorbate coverage	$E_{int}(\theta_i)[eV]$	Formation energy [eV]	Frequencies [cm^{-1}]
OH-H	0.25	None	0.00	0.08	0.31	3734.7, 845.0, 535.1, 512.0, 420.6, 361.0, 267.8, 185.1
OH-H	0.25	CO	0.25	-0.16	0.28	3734.7, 845.0, 535.1, 512.0, 420.6, 361.0, 267.8, 185.1
OH-H	0.25	CO	0.75	-0.51	0.58	3734.7, 845.0, 535.1, 512.0, 420.6, 361.0, 267.8, 185.1
O-OHH	0.25	None	0.00	-0.01	-0.03	3872.4, 1475.2, 1281.9, 755.4, 650.7, 443.2, 420.6, 354.7, 256.0, 163.1, 85.9
O-OHH	0.25	CO	0.25	-0.21	0.09	3872.4, 1475.2, 1281.9, 755.4, 650.7, 443.2, 420.6, 354.7, 256.0, 163.1, 85.9
O-OHH	0.25	CO	0.50	-0.40	0.14	3872.4, 1475.2, 1281.9, 755.4, 650.7, 443.2, 420.6, 354.7, 256.0, 163.1, 85.9
O-OHH	0.25	CO	0.75	-0.59	0.23	3872.4, 1475.2, 1281.9, 755.4, 650.7, 443.2, 420.6, 354.7, 256.0, 163.1, 85.9
CO-OH	0.25	None	0.00	-0.15	-0.56	3760.0, 1960.1, 819.9, 585.9, 347.2, 343.1, 258.2, 185.6, 138.1, 50.0, 50.0

Adsorbate	Coverage	Coadsorbate	Coadsorbate coverage	$E_{int}(\theta_i)[eV]$	Formation energy [eV]	Frequencies [cm^{-1}]
CO-OH	0.25	CO	0.50	-0.57	-0.53	3760.0, 1960.1, 819.9, 585.9, 347.2, 343.1, 258.2, 185.6, 138.1, 50.0, 50.0
CO-OH	0.25	CO	0.75	-0.74	-0.37	3760.0, 1960.1, 819.9, 585.9, 347.2, 343.1, 258.2, 185.6, 138.1, 50.0, 50.0
CO-HO	0.25	None	0.00	-0.11	-0.44	3636.6, 1805.2, 1107.0, 694.3, 494.5, 393.2, 315.2, 249.9, 164.6, 68.4, 50.0
CO-HO	0.25	CO	0.50	-0.48	-0.17	3636.6, 1805.2, 1107.0, 694.3, 494.5, 393.2, 315.2, 249.9, 164.6, 68.4, 50.0
CO-HO	0.25	CO	0.75	-0.66	-0.04	3636.6, 1805.2, 1107.0, 694.3, 494.5, 393.2, 315.2, 249.9, 164.6, 68.4, 50.0
COO-OHH	0.25	None	0.00	-0.26	-1.00	3818.2, 2168.8, 1629.5, 1464.5, 1199.4, 1133.4, 742.8, 677.6, 415.6, 364.7, 343.6, 259.2, 217.9, 162.6, 128.1, 90.9, 65.9
COO-OHH	0.25	CO	0.25	-0.44	-0.85	3818.2, 2168.8, 1629.5, 1464.5, 1199.4, 1133.4, 742.8, 677.6, 415.6, 364.7, 343.6, 259.2, 217.9, 162.6, 128.1, 90.9, 65.9

Adsorbate	Coverage	Coadsorbate	Coadsorbate coverage	$E_{int}(\theta_i)[eV]$	Formation energy [eV]	Frequencies [cm^{-1}]
COO-OHH	0.25	CO	0.50	-0.62	-0.70	3818.2, 2168.8, 1629.5, 1464.5, 1199.4, 1133.4, 742.8, 677.6, 415.6, 364.7, 343.6, 259.2, 217.9, 162.6, 128.1, 90.9, 65.9
COO-OHH	0.25	CO	0.75	-0.77	-0.50	3818.2, 2168.8, 1629.5, 1464.5, 1199.4, 1133.4, 742.8, 677.6, 415.6, 364.7, 343.6, 259.2, 217.9, 162.6, 128.1, 90.9, 65.9
HCO-O	0.25	None	0.00	0.12	0.47	2983.4, 1775.1, 1189.0, 740.1, 497.4, 374.4, 338.5, 246.2, 217.3, 136.3, 50.0
HCO-O	0.25	CO	0.25	-0.07	0.66	2983.4, 1775.1, 1189.0, 740.1, 497.4, 374.4, 338.5, 246.2, 217.3, 136.3, 50.0
HCO-O	0.25	CO	0.50	-0.29	0.60	2983.4, 1775.1, 1189.0, 740.1, 497.4, 374.4, 338.5, 246.2, 217.3, 136.3, 50.0
H-H	0.25	None	0.00	0.13	0.54	1328.6, 983.5, 566.9, 361.8, 317.5
H-H	0.25	CO	0.25	-0.08	0.58	1328.6, 983.5, 566.9, 361.8, 317.5
H-H	0.25	CO	1.00	-0.67	0.78	1328.6, 983.5, 566.9, 361.8, 317.5
O-H	0.25	None	0.00	0.33	1.30	728.0, 666.5, 504.8, 395.9, 269.9
O-H	0.25	CO	0.75	-0.26	1.58	728.0, 666.5, 504.8, 395.9, 269.9

Adsorbate	Coverage	Coadsorbate	Coadsorbate coverage	$E_{int}(\theta_i)[eV]$	Formation energy [eV]	Frequencies [cm^{-1}]
O-H	0.25	CO	1.00	-0.43	1.74	728.0, 666.5, 504.8, 395.9, 269.9
CO-O	0.25	None	0.00	0.08	0.33	1963.8, 568.2, 353.2, 347.3, 301.4, 248.6, 116.2, 50.0
CO-O	0.25	CO	0.25	-0.15	0.35	1963.8, 568.2, 353.2, 347.3, 301.4, 248.6, 116.2, 50.0
CO-O	0.25	CO	0.50	-0.30	0.52	1963.8, 568.2, 353.2, 347.3, 301.4, 248.6, 116.2, 50.0
CO-O	0.25	CO	0.75	-0.49	0.64	1963.8, 568.2, 353.2, 347.3, 301.4, 248.6, 116.2, 50.0
COO-H	0.25	None	0.00	0.09	0.37	1760.1, 1108.9, 885.7, 609.8, 511.5, 483.1, 280.5, 144.7, 83.1, 71.9, 50.0
COO-H	0.25	CO	0.25	-0.14	0.36	1760.1, 1108.9, 885.7, 609.8, 511.5, 483.1, 280.5, 144.7, 83.1, 71.9, 50.0
COO-H	0.25	CO	0.75	-0.53	0.50	1760.1, 1108.9, 885.7, 609.8, 511.5, 483.1, 280.5, 144.7, 83.1, 71.9, 50.0
CO-H	0.25	None	0.00	0.04	0.14	1891.0, 1636.2, 1004.2, 333.6, 266.3, 240.2, 50.0, 50.0

Adsorbate	Coverage	Coadsorbate	Coadsorbate coverage	$E_{int}(\theta_i)[eV]$	Formation energy [eV]	Frequencies [cm^{-1}]
CO-H	0.25	CO	0.25	-0.20	0.12	1891.0, 1636.2, 1004.2, 333.6, 266.3, 240.2, 50.0, 50.0
CO-H	0.25	CO	0.50	-0.40	0.16	1891.0, 1636.2, 1004.2, 333.6, 266.3, 240.2, 50.0, 50.0
H-COO	0.25	None	0.00	-0.15	-0.60	2122.2, 1511.2, 1134.4, 750.0, 703.6, 468.2, 265.8, 82.8, 55.1, 50.0, 50.0
H-COO	0.25	CO	0.25	-0.38	-0.61	2122.2, 1511.2, 1134.4, 750.0, 703.6, 468.2, 265.8, 82.8, 55.1, 50.0, 50.0
H-COO	0.25	CO	0.50	-0.58	-0.56	2122.2, 1511.2, 1134.4, 750.0, 703.6, 468.2, 265.8, 82.8, 55.1, 50.0, 50.0
H-	0.05	None	0.00	0.00	0.06	1136.3, 829.5
H	0.05	None	0.00	-0.00	-0.08	1014.1, 893.4, 746.6

S6.14 Cu_3 Elementary Steps

These are the elementary steps used in the microkinetic modeling for Cu_3 cluster.

$$*_s + CO_{(g)} \leftrightarrow CO^{*_s} \tag{39}$$

$$*_s + H_2O_{(g)} \leftrightarrow H_2O^{*_s} \tag{40}$$

$$*_s + CO_{2(g)} \leftrightarrow CO_2^{*_s} \tag{41}$$

$$H_2O^{*_s} + *_t \leftrightarrow OH{-}H^{*_s} + *_t \rightarrow H^{*_t} + OH^{*_s} \tag{42}$$

$$OH^{*_s} + *_t \leftrightarrow O{-}H^{*_s} + *_t \rightarrow O^{*_s} + H^{*_t} \tag{43}$$

$$OH^{*_s} + OH^{*_s} \leftrightarrow O{-}OHH^{*_s} + *_s \rightarrow H_2O^{*_s} + O^{*_s} \tag{44}$$

$$CO^{*_s} + O^{*_s} \leftrightarrow CO{-}O^{*_s} + *_s \rightarrow CO_2^{*_s} + *_s \tag{45}$$

$$CO^{*_s} + OH^{*_s} \leftrightarrow CO{-}OH^{*_s} + *_s \rightarrow COOH^{*_s} + *_s \tag{46}$$

$$COOH^{*_s} \leftrightarrow CO{-}HO^{*_s} \rightarrow COHO^{*_s} \tag{47}$$

$$COHO^{*_s} + *_s \leftrightarrow COO{-}H^{*_s} + *_s \rightarrow CO_2^{*_s} + H^{*_s} \tag{48}$$

$$H^{*_s} + H^{*_t} \leftrightarrow H{-}H^{*_s} + *_t \rightarrow H_{2(g)} + *_s + *_t \tag{49}$$

$$H^{*_t} + *_s \leftrightarrow H{-}^{*_t} + *_s \rightarrow H^{*_s} + *_t \tag{50}$$

S6.15 Cu_3 Interaction Parameters

All unlisted $\epsilon_{i,j}$ in Table S12 are assumed to be zero.

Table S12: Lateral interaction parameters $\epsilon_{i,j}$ on Cu_3.

i	j	$\epsilon_{i,j}$
CO	CO	0.18
CO	CO_2	-0.82
CO	COHO	-0.34
CO	COOH	0.39
CO	H_2O	-0.24
CO	H	-0.29
CO	OH	0.24
CO	O	0.05
CO	CO-HO	0.19
CO	CO-OH	1.32
CO	CO-O	1.22
CO	COO-H	0.32
CO	H-H	0.48
CO	O-H	0.52
CO	O-OHH	2.12
CO	OH-H	0.09

S6.16 Cu_3 Energies and Frequencies

Table S13 summarizes the adsorbates, coadsorbates, their coverages, integral formation energies (E_{int}), formation energies, and vibrational frequencies on Cu_3.

Table S13: Adsorbates, coadsorbates, formation energies, and frequencies for Cu_3.

Adsorbate	Coverage	Coadsorbate	Coadsorbate coverage	$E_{int}(\theta_i)[eV]$	Formation energy [eV]	Frequencies [cm^{-1}]
CO(g)	0.00	None	0.00	0.00	0.00	2165.5
CO2(g)	0.00	None	0.00	-0.84	-0.84	2401.6, 1328.9, 642.0, 642.0
H2(g)	0.00	None	0.00	0.00	0.00	4403.9
H2O(g)	0.00	None	0.00	0.00	0.00	3898.9, 3794.3, 1580.8
CO	0.33	None	0.00	-0.31	-0.93	2079.8, 330.0, 276.6, 237.4, 50.0, 50.0
CO	0.67	None	0.00	-0.60	-0.89	2079.8, 330.0, 276.6, 237.4, 50.0, 50.0
CO	1.00	None	0.00	-0.88	-0.84	2079.8, 330.0, 276.6, 237.4, 50.0, 50.0
H2O	0.33	None	0.00	-0.14	-0.41	3824.4, 3717.9, 1576.3, 490.4, 404.3, 163.6, 125.7, 50.0, 50.0
H2O	0.33	CO	0.33	-0.46	-0.44	3824.4, 3717.9, 1576.3, 490.4, 404.3, 163.6, 125.7, 50.0, 50.0
H2O	0.33	CO	0.67	-0.75	-0.46	3824.4, 3717.9, 1576.3, 490.4, 404.3, 163.6, 125.7, 50.0, 50.0
OH	0.33	None	0.00	-0.16	-0.47	3769.7, 629.4, 515.9, 392.5, 253.6, 76.9
OH	0.33	CO	0.67	-0.70	-0.30	3769.7, 629.4, 515.9, 392.5, 253.6, 76.9

Adsorbate	Coverage	Coadsorbate	Coadsorbate coverage	$E_{int}(\theta_i)[eV]$	Formation energy [eV]	Frequencies [cm^{-1}]
OH	0.33	CO	1.00	-0.99	-0.34	3769.7, 629.4, 515.9, 392.5, 253.6, 76.9
O	0.33	None	0.00	0.05	0.15	454.4, 348.5, 348.4
O	0.33	CO	0.33	-0.26	0.16	454.4, 348.5, 348.4
O	0.33	CO	1.00	-0.81	0.21	454.4, 348.5, 348.4
COOH	0.33	None	0.00	-0.32	-0.96	3601.3, 1797.5, 1115.6, 732.2, 483.9, 395.8, 293.0, 282.9, 232.6, 130.8, 58.9, 50.0
COOH	0.33	CO	0.33	-0.65	-1.02	3601.3, 1797.5, 1115.6, 732.2, 483.9, 395.8, 293.0, 282.9, 232.6, 130.8, 58.9, 50.0
COOH	0.33	CO	0.67	-0.87	-0.82	3601.3, 1797.5, 1115.6, 732.2, 483.9, 395.8, 293.0, 282.9, 232.6, 130.8, 58.9, 50.0
COHO	0.33	None	0.00	-0.22	-0.67	3640.5, 1738.3, 1272.8, 994.6, 629.1, 622.5, 406.3, 243.0, 199.1, 50.7, 50.0, 50.0
COHO	0.33	CO	0.33	-0.55	-0.73	3640.5, 1738.3, 1272.8, 994.6, 629.1, 622.5, 406.3, 243.0, 199.1, 50.7, 50.0, 50.0

Adsorbate	Coverage	Coadsorbate	Coadsorbate coverage	$E_{int}(\theta_i)[eV]$	Formation energy [eV]	Frequencies [cm^{-1}]
COHO	0.33	CO	0.67	-0.85	-0.75	3640.5, 1738.3, 1272.8, 994.6, 629.1, 622.5, 406.3, 243.0, 199.1, 50.7, 50.0, 50.0
CHO	0.33	None	0.00	-0.20	-0.60	2659.6, 1633.8, 1136.6, 704.8, 452.9, 246.3, 96.4, 51.8, 50.0
CHO	0.33	CO	0.33	-0.51	-0.60	2659.6, 1633.8, 1136.6, 704.8, 452.9, 246.3, 96.4, 51.8, 50.0
CHO	0.33	CO	0.67	-0.80	-0.59	2659.6, 1633.8, 1136.6, 704.8, 452.9, 246.3, 96.4, 51.8, 50.0
HCOO	0.33	None	0.00	-0.60	-1.79	2974.1, 1535.5, 1333.4, 1327.0, 1004.9, 753.0, 334.7, 309.6, 278.1, 104.7, 94.2, 50.0
HCOO	0.33	CO	0.33	-1.05	-2.22	2974.1, 1535.5, 1333.4, 1327.0, 1004.9, 753.0, 334.7, 309.6, 278.1, 104.7, 94.2, 50.0
CO2	0.33	None	0.00	-0.35	-1.04	2372.8, 1319.2, 595.9, 574.6, 77.0, 66.0, 50.0, 50.0, 50.0

Adsorbate	Coverage	Coadsorbate	Coadsorbate coverage	$E_{int}(\theta_i)[eV]$	Formation energy [eV]	Frequencies [cm^{-1}]
CO2	0.33	CO	0.33	-0.68	-1.10	2372.8, 1319.2, 595.9, 574.6, 77.0, 66.0, 50.0, 50.0, 50.0
H	0.33	None	0.00	-0.11	-0.32	1037.2, 671.2, 666.6
H	0.33	CO	0.67	-0.75	-0.44	1037.2, 671.2, 666.6
H	0.33	CO	1.00	-1.03	-0.45	1037.2, 671.2, 666.6
OH-H	0.33	None	0.00	0.14	0.43	3752.5, 844.7, 567.9, 526.3, 453.6, 342.0, 234.9, 163.0
OH-H	0.33	CO	0.33	-0.17	0.43	3752.5, 844.7, 567.9, 526.3, 453.6, 342.0, 234.9, 163.0
OH-H	0.33	CO	0.67	-0.44	0.48	3752.5, 844.7, 567.9, 526.3, 453.6, 342.0, 234.9, 163.0
O-H	0.33	None	0.00	0.37	1.12	912.3, 841.3, 413.4, 280.8, 278.9
O-H	0.33	CO	0.33	0.08	1.18	912.3, 841.3, 413.4, 280.8, 278.9
O-H	0.33	CO	0.67	-0.17	1.30	912.3, 841.3, 413.4, 280.8, 278.9
O-OHH	0.33	None	0.00	-0.08	-0.23	3795.0, 2900.3, 1585.6, 1084.9, 621.6, 527.3, 436.4, 382.9, 308.7, 237.2, 62.6

Adsorbate	Coverage	Coadsorbate	Coadsorbate coverage	$E_{int}(\theta_i)[eV]$	Formation energy [eV]	Frequencies [cm^{-1}]
O-OHH	0.33	CO	0.33	-0.33	-0.07	3795.0, 2900.3, 1585.6, 1084.9, 621.6, 527.3, 436.4, 382.9, 308.7, 237.2, 62.6
O-OHH	0.33	CO	0.67	-0.46	0.43	3795.0, 2900.3, 1585.6, 1084.9, 621.6, 527.3, 436.4, 382.9, 308.7, 237.2, 62.6
CO-O	0.33	None	0.00	-0.02	-0.04	2000.6, 548.5, 371.7, 354.7, 309.7, 251.7, 128.2, 50.0
CO-O	0.33	CO	0.33	-0.26	0.17	2000.6, 548.5, 371.7, 354.7, 309.7, 251.7, 128.2, 50.0
CO-O	0.33	CO	0.67	-0.49	0.35	2000.6, 548.5, 371.7, 354.7, 309.7, 251.7, 128.2, 50.0
CO-OH	0.33	None	0.00	-0.22	-0.66	3686.6, 1908.6, 877.8, 629.8, 392.7, 334.0, 282.9, 241.5, 137.9, 70.4, 50.0
CO-OH	0.33	CO	0.33	-0.52	-0.62	3686.6, 1908.6, 877.8, 629.8, 392.7, 334.0, 282.9, 241.5, 137.9, 70.4, 50.0
CO-OH	0.33	CO	0.67	-0.68	-0.24	3686.6, 1908.6, 877.8, 629.8, 392.7, 334.0, 282.9, 241.5, 137.9, 70.4, 50.0

Adsorbate	Coverage	Coadsorbate	Coadsorbate coverage	$E_{int}(\theta_i)[eV]$	Formation energy [eV]	Frequencies [cm^{-1}]
CO-HO	0.33	None	0.00	-0.09	-0.26	3684.3, 1750.3, 1051.2, 732.5, 585.3, 389.3, 260.0, 185.0, 73.8, 50.0, 50.0
CO-HO	0.33	CO	0.33	-0.39	-0.24	3684.3, 1750.3, 1051.2, 732.5, 585.3, 389.3, 260.0, 185.0, 73.8, 50.0, 50.0
CO-HO	0.33	CO	0.67	-0.66	-0.18	3684.3, 1750.3, 1051.2, 732.5, 585.3, 389.3, 260.0, 185.0, 73.8, 50.0, 50.0
COO-H	0.33	None	0.00	0.14	0.43	1767.3, 1109.8, 842.1, 619.0, 550.6, 489.6, 272.7, 158.2, 77.1, 54.2, 50.0
COO-H	0.33	CO	0.33	-0.15	0.49	1767.3, 1109.8, 842.1, 619.0, 550.6, 489.6, 272.7, 158.2, 77.1, 54.2, 50.0
COO-H	0.33	CO	0.67	-0.42	0.55	1767.3, 1109.8, 842.1, 619.0, 550.6, 489.6, 272.7, 158.2, 77.1, 54.2, 50.0
COO-OHH	0.33	None	0.00	-0.29	-0.88	3802.0, 1679.7, 1569.5, 1288.0, 1085.9, 921.9, 794.6, 530.4, 517.9, 389.7, 301.1, 249.5, 174.3, 133.9, 100.4, 79.0, 50.0

Adsorbate	Coverage	Coadsorbate	Coadsorbate coverage	$E_{int}(\theta_i)[eV]$	Formation energy [eV]	Frequencies [cm^{-1}]
COO-OHH	0.33	CO	0.33	-0.59	-0.84	3802.0, 1679.7, 1569.5, 1288.0, 1085.9, 921.9, 794.6, 530.4, 517.9, 389.7, 301.1, 249.5, 174.3, 133.9, 100.4, 79.0, 50.0
COO-OHH	0.33	CO	0.67	-0.88	-0.84	3802.0, 1679.7, 1569.5, 1288.0, 1085.9, 921.9, 794.6, 530.4, 517.9, 389.7, 301.1, 249.5, 174.3, 133.9, 100.4, 79.0, 50.0
CO-H	0.33	None	0.00	-0.05	-0.13	2508.4, 1633.2, 1253.3, 502.4, 276.5, 161.7, 75.7, 50.0
CO-H	0.33	CO	0.33	-0.35	-0.10	2508.4, 1633.2, 1253.3, 502.4, 276.5, 161.7, 75.7, 50.0
CO-H	0.33	CO	0.67	-0.56	0.14	2508.4, 1633.2, 1253.3, 502.4, 276.5, 161.7, 75.7, 50.0
HCO-O	0.33	None	0.00	0.04	0.12	2942.2, 1768.6, 1182.3, 722.3, 489.2, 380.7, 358.3, 264.4, 226.1, 136.4, 50.0
HCO-O	0.33	CO	0.33	-0.23	0.24	2942.2, 1768.6, 1182.3, 722.3, 489.2, 380.7, 358.3, 264.4, 226.1, 136.4, 50.0

Adsorbate	Coverage	Coadsorbate	Coadsorbate coverage	$E_{int}(\theta_i)[eV]$	Formation energy [eV]	Frequencies [cm^{-1}]
H-COO	0.33	None	0.00	-0.29	-0.88	1965.4, 1260.4, 1153.8, 1046.5, 826.5, 493.4, 269.7, 185.9, 97.1, 78.2, 50.0
H-COO	0.33	CO	0.33	-0.60	-0.86	1965.4, 1260.4, 1153.8, 1046.5, 826.5, 493.4, 269.7, 185.9, 97.1, 78.2, 50.0
H-H	0.33	None	0.00	0.16	0.49	1341.8, 980.4, 400.9, 376.8, 172.0
H-H	0.33	CO	0.33	-0.11	0.60	1341.8, 980.4, 400.9, 376.8, 172.0
H-H	0.33	CO	1.00	-0.62	0.79	1341.8, 980.4, 400.9, 376.8, 172.0
H2O	0.06	None	0.00	-0.02	-0.37	3758.2, 3664.9, 1551.3, 497.3, 418.3, 142.6, 56.5, 50.0
H	0.06	None	0.00	-0.00	-0.02	1022.1, 917.0, 740.4
OH	0.06	None	0.00	0.01	0.18	3749.3, 706.3, 551.9, 347.4, 202.8, 115.7
H-	0.06	None	0.00	0.00	0.06	1122.1, 969.4
OH-	0.06	None	0.00	0.02	0.28	3681.3, 435.7, 318.4, 241.5

References

(1) Abild-Pedersen, F.; Andersson, M. CO adsorption energies on metals with correction for high coordination adsorption sites – A density functional study. *Surface Science* **2007**, *601*, 1747–1753.

(2) Halim, H. H.; Ueda, R.; Morikawa, Y. Machine learning molecular dynamics simulation of CO-driven formation of Cu clusters on the Cu(111) surface. *Journal of Physics: Condensed Matter* **2023**, *35*, 495001.

(3) Thompson, A. P.; Aktulga, H. M.; Berger, R.; Bolintineanu, D. S.; Brown, W. M.; Crozier, P. S.; in 't Veld, P. J.; Kohlmeyer, A.; Moore, S. G.; Nguyen, T. D.; Shan, R.; Stevens, M. J.; Tranchida, J.; Trott, C.; Plimpton, S. J. LAMMPS - a flexible simulation tool for particle-based materials modeling at the atomic, meso, and continuum scales. *Computer Physics Communications* **2022**, *271*.

(4) Tribello, G. A.; Bonomi, M.; Branduardi, D.; Camilloni, C.; Bussi, G. PLUMED 2: New feathers for an old bird. *Computer Physics Communications* **2014**, *185*, 604–613.

(5) The PLUMED consortium. Promoting transparency and reproducibility in enhanced molecular simulations. *Nature Methods* **2019**, *16*, 670–673.

(6) Hjorth Larsen, A. et al. The atomic simulation environment—a Python library for working with atoms. *Journal of Physics: Condensed Matter* **2017**, *29*, 273002.

(7) Bartók, A. P.; Payne, M. C.; Kondor, R.; Csányi, G. Gaussian approximation potentials: The accuracy of quantum mechanics, without the electrons. *Physical Review Letters* **2010**, *104*.

(8) Caro, M. A. Optimizing many-body atomic descriptors for enhanced computational performance of machine learning based interatomic potentials. *Physical Review B* **2019**, *100*.

(9) Kumar, S.; Rosenberg, J. M.; Bouzida, D.; Swendsen, R. H.; Kollman, P. A. THE weighted histogram analysis method for free-energy calculations on biomolecules. I. The method. *Journal of Computational Chemistry* **1992**, *13*, 1011–1021.

(10) Barducci, A.; Bussi, G.; Parrinello, M. Well-tempered metadynamics: A smoothly converging and tunable free-energy method. *Physical Review Letters* **2008**, *100*.

(11) Medford, A. J.; Shi, C.; Hoffmann, M. J.; Lausche, A. C.; Fitzgibbon, S. R.; Bligaard, T.; Nørskov, J. K. CatMAP: A Software Package for Descriptor-Based Microkinetic Mapping of Catalytic Trends. *Catalysis Letters* **2015**, *145*, 794–807.

(12) Vijay, S.; H. Heenen, H.; Singh, A. R.; Chan, K.; Voss, J. Number of sites-based solver for determining coverages from steady-state mean-field micro-kinetic models. *Journal of Computational Chemistry* **2024**, *45*, 546–551.

(13) Yang, N.; Medford, A. J.; Liu, X.; Studt, F.; Bligaard, T.; Bent, S. F.; Nørskov, J. K. Intrinsic Selectivity and Structure Sensitivity of Rhodium Catalysts for C2+ Oxygenate Production. *Journal of the American Chemical Society* **2016**, *138*, 3705–3714.

(14) Campbell, C.; Daube, K. A surface science investigation of the water-gas shift reaction on Cu(111). *Journal of Catalysis* **1987**, *104*, 109–119.